Discovery and Pharmacological Study of a Novel GPR142 Antagonist, CLP-3094 and a Metal Modulator, Zn ion

著者	Michiko MURAKOSHI
year	2017
その他のタイトル	GPR142における金属モジュレーターおよびアンタゴニストの同定と免疫抑制機能に関する研究
学位授与大学	筑波大学 (University of Tsukuba)
学位授与年度	2016
報告番号	12102甲第8160号
URL	http://hdl.handle.net/2241/00147671

Discovery and Pharmacological Study of a Novel GPR142 Antagonist, CLP-3094 and a Metal Modulator, Zn ion

January 2017

Michiko MURAKOSHI

Discovery and Pharmacological Study of a Novel GPR142 Antagonist, CLP-3094 and a Metal Modulator, Zn ion

A Dissertation Submitted to

the Graduate School of Life and Environmental Sciences,

the University of Tsukuba

in Partial Fulfillment of the Requirements

for the Degree of Doctor of Philosophy in Biotechnology

(Doctoral Program in Life Sciences and Bioengineering)

Michiko MURAKOSHI

Abbreviations

AC	adenylate cyclase
cAMP	cyclic adenosine monophosphate
BSA	bovine serum albumin
CII	type II collagen
CAIA	anti-type II collagen (CII) antibody-induced arthritis
CFA	complete Freund's adjuvant
CIA	collagen-induced arthritis
CPS	counts per second
CPM	counts per minutes
DMEM	Dulbecco's modified eagle medium
DSS	dextran sulfate sodium
EDTA	ethylenediaminetetraacetic acid
ESI	electrospray ionization
FBS	fetal bovine serum
Fr.	fraction
GSIS	glucose-stimulated insulin secretion
GPCR	G-protein coupled receptor

GPR142	G protein-coupled receptor 142
HBSS	Hanks' balanced salt solution
HEPES	4-(2-hydroxyethyl)-1-piperazineethanesulfonic acid
HPLC	high performance liquid chromatography、
HTS	high throughput screening
IFN	interferon
IL	interleukin
i.p.	intraperitoneal administration
IP(s)	inositol phosphate(s)
IP3	inositol 1,4,5-trishosphate
i.v.	intravenous administration
KO	knock out
LPS	lipopolysaccharide
LC/MS	liquid chromatography / mass spectrometry
mAb	monoclonal antibody
MEM	minimum essential media
mRNA	messenger ribonucleic acid
Mw.	molecular weight

PBS	phosphate buffered saline
Pen	penicillin
PLC	phospholipase C
TBS	tris buffered saline
TFA	trifluoroacetic acid
TNF	tumor necrosis factor
Trp	tryptophan (L-Tryptophan)
RA	rheumatoid arthritis
RT-PCR	reverse transcription polymerase chain reaction
SD	standard deviation
Strep	streptomycin
WT	wild type

Contents

CHAPTER 1

Preface

GPCR Research in Drug Discovery

G protein-coupled receptors (GPCRs), also known as seven-transmembrane (7-TM) receptors, are one of the largest families of membrane proteins. GPCRs sense extracellular stimuli (bioactive peptides, including extracellular hormones and neurotransmitters, nucleic acids, pH, etc.) and induce various cellular responses by activating intracellular signal pathways.

GPCR signals are transmitted through a trimeric protein called G protein, which consists of three subunits, Gα, Gβ, and Gγ. When a ligand binds to a GPCR, it causes conformational changes to the GPCR and the consequent activation of its associated G protein by exchanging GDP for GTP. Together with the bound GTP, the α subunit dissociates from the β and γ subunits and activates intracellular signal pathways depending on the subtype of the α unit. Dissociated GTP-bound Gα as well as β and γ subunits modulate various effector functions, and following spontaneous hydrolysis of GTP to GDP result in reassociation of GDP-bound Gα with Gβγ.

The functional diversity of the G protein mediated signaling depends on the fact that there are numerous subtypes of G proteins. The basic characteristics of the heterotrimeric G protein are regulated by the subtype of the α-subunit, which is divided into four families: Gαq/Gα11, Gαi/Gαo, Gαs, and Gα12/Gα13.

Although there are many exceptions, the receptor-G protein combinations are classified into three basic classes that define the intercellular responses caused by the ligand-dependent receptor activation (Figure 1) (Ref. 1).

Figure 1. Typical patterns of receptor/G protein coupling

The Gα proteins of the Gq/G11 family couple to β-isoforms of phospholipase C (Ref. 2). The Gα proteins of the Gi/Go family are expressed ubiquitously and the α-subunits of the Gi subtype have been shown to inhibit adenylyl cyclases (Ref. 3). Gαi signaling has also been reported to activate MAP kinase and promote cell proliferation. In contrast, the widely expressing G protein, Gαs couples to adenylyl cyclase and mediates receptor-activation dependent adenylyl cyclase activation, resulting in increases in the intracellular cAMP concentrations. Those of the G12/G13 family are expressed ubiquitously, and are reported to be activated by their coupling to Gαq/Gα11 (Ref. 4). Another important function of Gα12 and Gα13 is their ability to induce various physiological functions, such as stress fiber formation and neurite retraction, by increasing the activity of the small GTPase RhoA (Ref. 5).

GPCRs are widely expressed in the body and play a physiological and pathophysiological role. Indeed, they are potential targets for drugs combating many diseases. Of the ~500 currently marketed drugs, greater than 30% are modulators of GPCR function (Figure 2) (Ref. 6). In the year 2000, 26 of the top 100 pharmaceutical products were the compounds targeting GPCRs. Their total sales were over US$23.5 billion which amounts to ~9% of total global pharmaceutical sales (Ref. 7), thus, GPCR is regarded as the most successful target class in drug discovery.

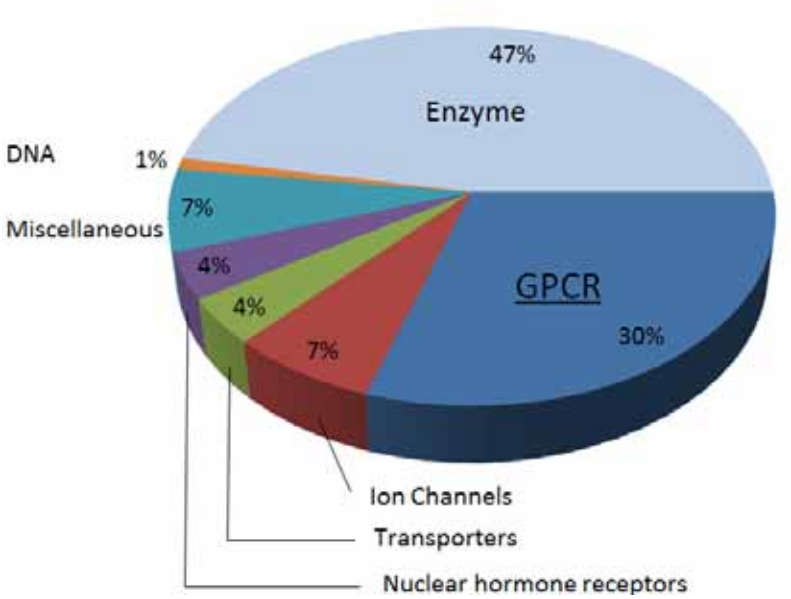

Figure 2. Marketed small-molecule drug targets by biochemical class [modified from reference 6]

Figure 2 shows the distribution of biochemical class of marketed drugs. Enzymes represent about half of the launched targets, whereas GPCRs account for 30%. All other classes, such as ion channels and transporters, accounts for less than a quarter of the launch target.

From the second half of the 1980s, the rush for discovery in GPCR research began with homology searches employing the genomic sequence and structural prediction (Ref. 8). As genetic information was clarified by the Human Genome Project, over 800 GPCRs were discovered by bioinformatics analysis (Ref. 9). On the other hand, GPCRs found by homology screening suffer from one obvious problem; these receptors are *orphan* receptors lacking information on their endogenous ligands (Ref. 10).

Ligand Fishing

Owing to the successful mapping of the human genome, the genes of approximately 350 nonolfactory GPCRs have been cloned. More than 100 GPCRs still remain as orphan receptors, for which the endogenous ligands are unknown (Ref. 9, 11). Moreover, discovering the agonists and antagonists for those GPCRs is important to drug discovery since more than 30% of all marketed drugs are targeting GPCRs (Ref. 6). Therefore, the identification of endogenous ligands of orphan GPCRs likely will promote the discovery of novel mechanisms of physiological function and new drug targets.

There are two approaches to researching target molecules: a reverse type and a forward type. In other words, to conduct research to explain phenomena from characteristics of the active compounds (forward type, classical approach), or to conduct research with known (or predicted to be) disease-related molecules as a starting point (reverse type) (Ref. 10). In this *reverse pharmacology*, the identification of a receptor sequence is followed by the corresponding ligand discovery. Physiological and pharmacological functions are subsequently examined, for example, using gene knockout or overexpression of the receptor. GPCR is a molecular target representing this reverse pharmacology approach.

Ligand fishing is one of the approaches for *de-orphanization*, which is the process to identify a natural ligand for an orphan GPCR. The first orphan GPCR that was used for de-orphanization was an opioid receptor-like one, identified by homology search with the opioid receptors (Ref. 12). Since then, novel peptides such as ghrelin, prolactin-releasing peptide, neuropeptides, prokineticins, and neuromedin S have been reported as natural ligands of orphan GPCRs. These successes showed the effectiveness of the approach to find novel ligands of orphan GPCRs. Therefore, the pharmaceutical industry has rushed into the ligand fishing race.

GPR142

GPR142 is a G-protein-coupled receptor (GPCR), identified through genome database mining as a class A (rhodopsin) G protein-coupled receptor (Ref. 13). Over-expression of mouse GPR142 in HEK293 and CHO-K1 cells was shown to lead to activation of NFAT and accumulation of inositol phosphate, suggesting that this GPCR is likely coupled to Gαq. GPR142 highly expressed in the pancreas and the immune system shares 50% amino acid identity with GPR139. Recently, ligands for GPR139, a GPR142-related receptor with 50% amino acid identity, were reported as the essential amino acids L-Tryptophan (Trp) and L-Phenylalanine (Phe) (Ref. 14). GPR142 was also found to be a receptor for aromatic amino acids, with Trp representing one of the most potent ligands with an EC_{50} value of 0.2mM to 1 mM (Ref. 15).

GPR139 has been relatively more well-studied than GPR142. In humans and mice, GPR139 is expressed specifically in distinct areas of the CNS, especially in the basal ganglia and the hypothalamus, which are involved in movement control, regulation of food intake and metabolism (Ref. 16, 17). To date, four groups have reported small molecule ligands for GPR139. GPR139 agonists were shown to reduce locomotor activity in rats and protect primary dopaminergic midbrain neurons against some neurotoxin (Ref. 18), suggesting GPR139 could be a potential target for treatment of Parkinson's disease.

A high expression level of GPR142 in pancreatic β-cells suggests that the receptor may play a role in the pathogenesis and development of diabetes. GPR142 is highly expressed in pancreatic islets, and Trp and its small molecule agonists (Figure 3) stimulated glucose-stimulated insulin secretion (GSIS) in the cultured islets as well as in the rodent in vivo model is dependent on GPR142 (Ref. 19)(Figure 4). In addition, GPR142 is expressed in intestine and stimulates Trp induced secretion of incretins glucagon, like peptide-1 (GLP-1) and glucose-dependent insulinotropic peptide (GIP).

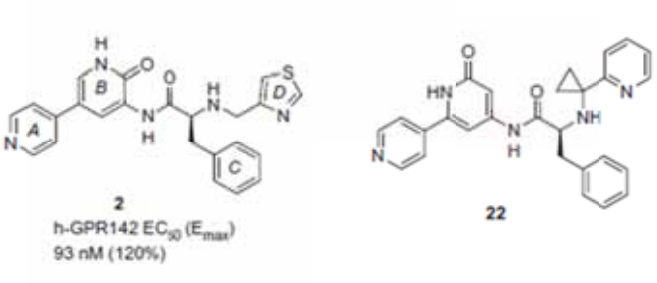

Figure 3. Reported GPR142 agonists

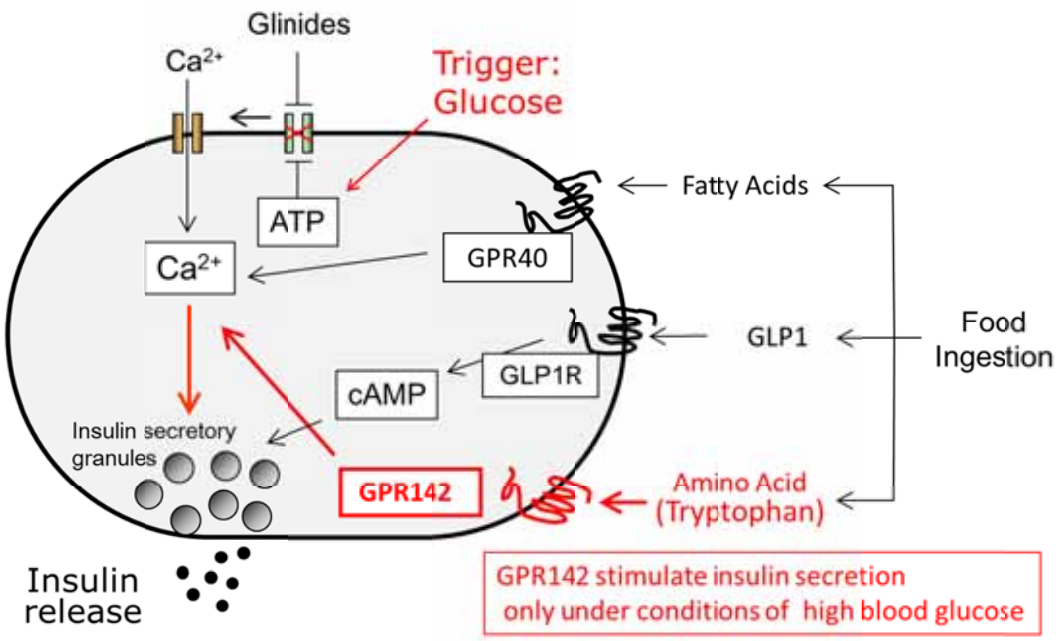

Figure 4. GPR142 as a novel target for Type 2 Diabetes

Proposed mechanism for stimulation of glucose-stimulated insulin secretion. The Gαs-coupled receptors, such as glucagonlike peptide 1 receptor (GLP1R), signal through adenylyl cyclase to increase cyclic AMP levels and activation of protein kinase A (PKA). The Gαq/11-coupled receptors, such as fatty acid receptor, GPR40, as well as GPR142 promote insulin secretion through activation of phospholipase C (PLC) ß-isoforms and the formation of inositol 1,4,5-triphosphate (IP_3), which leads to the release of Ca^{2+} from intracellular stores and Ca^{2+}-mediated vesicle exocytosis.

Insulin secretion is accelerated by the activation of PKA or by elevation of Ca^{2+} levels through the voltage-dependent Ca^{2+} channel.

On the other hand, GPR142 is highly expressed in immune cells as well as in pancreatic β-cells. In addition, the ligand of GPR142, Trp, and its metabolites, serotonin and kynurenine, are known to play important roles in inflammation (Ref. 20, 21), suggesting the receptor may play a role in inflammatory diseases.

Chronic Inflammatory Diseases

Inflammation, one of the important physiological defense mechanisms against infections such as viruses or bacteria, is a biological reaction essential to maintaining the healthy state. However, once inflammation comes to be chronic, it sometimes leads to the development of intractable diseases, such as autoimmune diseases; as a result, chronic inflammation has been recognized as a difficult disease group. In recent years, inflammatory diseases, including autoimmune diseases, have shown an increasing trend. This is due to rapid changes in the external environment, such as increases of stress, complex pollution or change of diet (Ref. 22).

Symptomatic treatment to block the overall inflammatory response using immunosuppressive drugs, including steroids, rather than definitive treatment to eliminate the cause of the chronic inflammation is still used in modern medical treatment. At the acute advanced stage, symptomatic treatment might be effective, but long-term administration can cause serious side effects, leading to a significant decrease of the health-related quality of life (QoL) of patients suffering autoimmune diseases. Thus, specific therapies based on molecular targets for autoimmune diseases are considerably expected to be developed.

Rheumatoid arthritis (RA) is a systemic and long-lasting autoimmune disease. It is reported that RA affects 0.5～1% of adults and ～50 per 100,000 people newly developing the condition each year (Ref. 23, 24). Although the cause of RA is not clear, it is thought that the combination of environmental and genetic background is involved. The underlying mechanism is the attacking of the joints by the auto immune system. This results in inflammation and thickening of the joint capsule and damage to bone and cartilage.

In developing RA, the abnormal growth of synovial membrane occurs in rheumatoid synovial tissue, while at the same time small blood vessels are formed in joints and the immune cells flow in from the blood. These immune cells secrete inflammatory mediators such as interleukin and prostaglandin, which are inflammatory cytokines; this leads to extensive angiogenesis and production of enzymes, such as matrix

metalloproteinases (MMPs) that cause tissue damage. On the other hand, in concert with the disease progression, neutrophil flows into the joint tissue and RA-specific inflammatory granulation tissue at the edges of the synovial lining (pannus) is formed (Ref. 25–28).

In the pathogenesis of RA, TNF-α plays a major role, but there still are many reports that other cytokines and chemical mediators are involved in inflammation in RA (Ref. 29–31). In RA patients, a deleterious cycle can occur where immune cells in the inflammatory joint capsule, both leucocyte-derived and lymphocyte-derived, are stimulated by cytokines, which leads to the production of more inflammatory cytokines, and results in an acute fulminant inflammatory reaction (Ref. 32).

Mouse Models of Chronic Inflammatory Diseases

Based on the method of induction, systemically induced mouse models of RA can be divided into 3 groups: those elicited by active immunization, those elicited by passive immunization, and those elicited by administration (Ref. 33).

Collagen-induced arthritis (CIA) is the archetypical model of RA induced by active immunization. Mice develop an acute to sub-acute single-phase erodible polyarthritis after immunization with collagen II. Type II collagen is the major collagen component in articular cartilage, and immuno-reactivity to type II collagen can be observed in some RA patients (Ref. 34). Many important features of human RA are recapitulated in mouse CIA, including the presence of rheumatoid factor or anticitrullinated peptide antibody (Ref. 35). A Th17-driven response is reported to be essential for the production of lesions (Ref. 36, 37). The effects of interferon γ are divergent with inhibitory as well as stimulatory effects on development of disease. Overall, however, interferon γ attenuates CIA (Ref. 38).

A widely used example of arthritis induced by passive immunization is the direct derivative of CIA, collagen antibody-induced arthritis (CAIA) (Ref. 39, 40).
One particular benefit of CAIA over CIA is that the model is amenable for use in strains or genotypes not suitable for CIA (Ref. 41, 42). CAIA, in contrast to CIA, is a fast model (peak disease within 8 days) and has a high degree of synchronicity in disease onset. CAIA requires immune complex formation and complement activation, but induction of arthritis is B-cell and T-cell independent and does therefore not recapitulate the complexity of immune and tissue remodeling responses during human RA (Ref. 43).

CIA mouse models are the most widely used disease models, which recapitulate the whole process of RA. CIA require $CD4^+$T-cells for the full induction of arthritis (Ref. 44) In contrast, T-cells or B-cells are not required for the induction of CAIA(Ref. 9) since T- and B-cell-deficient mice can induce CAIA effectively.
The contribution of inflammatory cytokines differs depending on the mouse disease condition used for evaluation (Table 1). It is indicated that $CD4^+$T-cells are required for

the initiation phase of CIA. $CD4^+$T-cells are not strictly necessary after the production of arthritogenic autoantibodies. The severity in the CAIA were augmented by adoptive transfer of a $CD4^+$T-cell(Ref. 43). It is important to choose the suitable disease model to evaluate the compound efficacy and to understand the underlying mechanism.

Table 1. The contribution of proinflammatory cytokines and lymphocytes to the development of mouse models of RA [modified from reference 40]

	IL-17A	IL-6	IL-1	TNF	$CD4^+$ T-cell	B-cell
CIA	+	+	++	+	+	+
CAIA	NR	-	++	++	-	-
IL-1Ra-deficient	++	-	NR	++	+	-
TNF-Tg	NR	-	++	++	-	-

-,Not required; +,partially required; ++,substantially required; NR, not reported.

Summary of the Thesis

In Chapter 2, I will discuss the GPR142 endogenous ligand fishing from porcine brain. I found an agonistic activity against GPR142 in extract of porcine brain, discriminated from L-Tryptophan, previously reported as a GPR142 natural ligand. Thus, I started fractionation of the extract to identify the compound that causes the agonistic activity.

Ion peak patterns observed in the mass spectrum of the active fraction, as well as HPLC retention time and UV spectrum of the active fraction were identical to those of standard $ZnCl_2$. From the analysis of the agonistic profile of the active fraction and $ZnCl_2$, it was concluded that the agonistic activity against GPR142 observed in porcine brain extract was caused by zinc ion. Further analysis revealed that zinc acts not as a ligand (agonist), but as modulator, which changes the properties of receptor activation by both natural and surrogate ligands.

In Chapter 3, to elucidate the physiological function of GPR142 especially in immune systems, we used GPR142 KO mice to pursue the possibility of GPR142 as a therapeutic target for inflammation diseases. GPR142 KO mice were protected from anti-type II collagen (CII) antibody-induced arthritis, thus we hypothesized that GPR142 could be a potential target for rheumatoid arthritis (RA) treatment.

Through an HTS campaign using an aequorin assay, a GPR142 selective antagonist with moderate potency, CLP-3094 was identified from in-house small molecule chemical compound libraries. Administration of CLP-3094 to CAIA mice dose-dependently reduced, by not much, the arthritis scores. CLP-3094-treated mice consistently displayed significantly lower severity of arthritis scores than vehicle treated mice, suggesting that the receptor also may play a role in the immune system.

In Chapter 4, this is described in the Concluding Remarks.

CHAPTER 2

GPR142 Endogenous Ligand Fishing From Porcine Brain

Abstract

In a search for endogenous ligands for GPR142, a neutral amino acid L-Tryptophan (Trp) was reported as a possible endogenous ligand from collaboration partner Amgen. On the other hand, I found an agonistic activity against GPR142 in extract of porcine brain, discriminated from Trp. Thus, I started fractionation of the extract to identify the compound that causes the agonistic activity.

A partially purified active fraction was obtained by a series of chromatography. The following two results indicated the presence of zinc ion in the active fraction. First, ion peak patterns observed in the mass spectrum of the active fraction were quite similar to the isotope peak pattern of Zn. Second, HPLC retention time and UV spectrum of the active fraction were identical to those of standard $ZnCl_2$. $ZnCl_2$ (EC_{50} = 1.4 μg/mL [10 μM]) and the active fraction (EC_{50} = 3 μg/mL) induced inositol phosphate (IP) accumulation at the similar concentration ranges in DMEM medium, and those accumulations were inhibited by adding EDTA. Therefore, it was concluded that the agonistic activity against GPR142 observed in porcine brain extract was caused by zinc ions.

Further analysis of the characteristics of zinc ions' activity against GPR142 activation was carried out more in more detail. First, I compared the effect of other metal ions on activation against GPR142. $MnCl_2$ and $AlCl_3$ also showed the agonistic activity, but both of them were weak compared to $ZnCl_2$.

Interestingly, zinc showed agonistic activity by inositol phosphates accumulation assay (IP assay) using cultured media as assay buffer, but not Hanks HEPES (H/H) buffer, meanwhile Trp showed both with the media and H/H buffer. Further analysis revealed that zinc acts not as a ligand (agonist), but as a modulator, which changes the properties of receptor activation by both natural and surrogate ligands.

Introduction

GPR142 is an orphan G-protein coupled receptor (GPCR), whose ligand has not yet been reported and thus its biological function is not clear. To identify a natural ligand for an orphan GPCR is important to clarify its physiological activity, and also to identify a novel target for drug discovery (Ref. 45). Discovery of ghrelin, a peptide ligand for growth hormone secretagogues receptor (GHS-R) purified from stomach (Ref. 46), accelerated the race for searching for the ligands (so-called ligand fishing) for orphan GPCRs.

GPR142 study started as a collaboration work with Amgen. Amgen reported Trp was purified from abdominal dropsy as a possible endogenous ligand for GPR142. However, its efficacy was very low (EC_{50} = 100 μg/mL). On the other hand, I found an agonistic activity against GPR142 in extract of porcine brain, discriminated from Trp. Furthermore, preliminary study for partially purified active fraction showed that the EC_{50} for the product was about 4 μg/mL, even stronger compared to the EC_{50} for Trp. Consequently, I decided to start the purification of active product from porcine brain to identify a novel natural ligand for GPR142.

Materials and Methods

Preparation of GPR142 cDNA and Expression in mammalian cell

Human GPR142 (hGPR142) receptor cDNA was cloned from a human spleen cDNA library and its sequence was confirmed (UniGene 1847355 - Hs.574368). The respective amplified fragment was subcloned into the pcDNA3.1 expression vector. Human embryonic kidney 293 (HEK293) cells were grown in DMEM supplemented with 10% FBS and penicillin-streptomycin. HEK293 cells were transfected with hGPR142 plasmid using Lipofectamine 2000 reagent (Invitrogen: Thermo Fisher Scientific Inc. Waltham, MA, USA).

Inositol Phosphates Accumulation Assay (IP Assay)

HEK293 cells were maintained in DMEM supplemented with 10% FBS and penicillin-streptomycin at 37 °C under a condition of 5% CO_2. Inositol phosphate accumulation was assayed as the incorporation of ^{3}H-myo-inositol as described (Ref. 47). Briefly, HEK293 cells were transiently transfected with human or mouse GPR142 containing plasmid using Lipofectamine 2000 reagent (Thermo Fisher Scientific Inc. (Waltham, MA, USA) and plated on culture plates the day previous to the assay. One day after transfection, cells were incubated over night with 10 μCi of myo-[3H(G)]-inositol (PerkinElmer, Inc., Waltham, MA, USA) in 10 mL of inositol free medium supplemented with 10% fetal bovine serum. Cells were stimulated with compounds in the presence of 10 mM LiCl for 90 min at 37 °C using cultured media (DMEM) as assay buffer before the addition of 20 mM ice-cold formic acid for extraction followed by incubation on ice for 30 min. The generated [^{3}H]-inositol phosphate was detected using RNA Binding YSi SPA Scintillation Beads (by interacting with primary phosphate groups in nucleotides and oligonucleotides, DNA and RNA.) (PerkinElmer, Inc., Waltham, MA, USA).

Aequorin Assay

The aequorin assay was performed as previously described (Ref. 48). Briefly, CHO-K1 cells were co-transfected with plasmids expressing pro-aequorin and mouse or human GPR142. Twenty-four hours later, transfected cells were harvested and incubated with Hank's balanced salt solution (HBSS, Gibco: Thermo Fisher Scientific

Inc. Waltham, MA, USA) containing 0.1% BSA (Sigma-Aldrich, St. Louis, MO, USA), and 1 μg/mL coelenterazine h (Molecular Probes: Thermo Fisher Scientific Inc. Waltham, MA, USA) for 2 h to 4 h. Aequorin luminescence was measured using an FDSS6000 (Hamamatsu Photonics K.K., Hamamatsu, Japan).

Preparation of the Extracts From Porcine Brain

Porcine brain (average size: 100 g per portion) purchased from Tokyo Shibaura Zouki K.K. was processed on the day of butchery or stored in the freezer at -20 °C.

Three portions of the brain were put in a Waring® Blender with 700 mL of 50 mM ammonium formate (pH 7.0). After 1 minute blending, samples were cooled on ice for 10 min and centrifuged (4,700*g*, 10 min, 4°C). Collected supernatant was added to 3 times the volume of methanol and mixed to leave at 4°C overnight. The next day, the mixture was centrifuged (4,700*g*, 10 min, 4°C), and the supernatant was concentrated using a rotary evaporator to remove methanol from the extract. Finally, the concentrate was subject to freeze-drying to obtain the porcine brain extract sample for ligand fishing. The dark brown extract sample obtained from 300 g (3 portions) porcine brain was about 4.2 g.

Purification of active fraction from porcine brain extracts

The procedure for purification of the agonistic component against GPR142 from porcine brain extract sample is shown in Figure 1.

The extract sample (70 g) from 5 kg brain was dissolved in D.W. and formic acid was added until the sample reached to pH 3.0. The supernatant was collected after centrifugation (2,000*g*, 15 min, 4°C).

A Diaion Sepabeads SP 207 column (500 mL) was equilibrated with 10 mM ammonium formate (pH 3.0, buffer-A), and the supernatant was loaded into the column and maintained for 8 h under a 4°C condition. The column was washed by 4.5 L of buffer-A. The flow-through and wash fractions were combined to 9 L and prepared to pH 9.0 with aqueous ammonia. Another Diaion Sepabeads SP 207 column (the second column, 500 mL) was equilibrated with 10 mM ammonium formate (pH 9.0, buffer-B), and the combined flow-through and wash fraction was loaded into the second column and maintained for 9 hours under a 4°C condition. The second column was washed by 3

L of buffer-B. Then, the second column was equilibrated to room temperature and adsorbed components in the column were desorbed by 3 L of buffer-A containing 10% acetone. The eluent was concentrated using a rotary evaporator to remove acetone and was then subjected to freeze-drying. A dark brown oily sample (126.2 mg) was obtained. This oily sample (70 mg) was diluted with 40 mL of 100 mM sodium acetate (pH 5.0, buffer-C), and the diluted sample was loaded into the 10 mL of Sigma-Aldrich CM Sephadex C-25 column equilibrated with buffer-C. The column was washed with 40 mL of buffer-C, 80 mL of buffer-C supplemented with 0.5 M NaCl and 80 mL of buffer-C supplemented with 1.0 M NaCl sequentially. Adsorbed components in the column were desorbed by 80 mL of buffer-C supplemented with 2.0 M NaCl to give Active Fraction 1 (EC_{50} = 3 μg/mL against GPR142).

The buffers used for the fractionation were prepared as follows:

Buffer-A: 380 μL (10 mmol) of ammonium formate was added to 1000 mL D.W. and prepared to pH 3.0 with 28% aqueous ammonia.

Buffer-B: 676 μL (10 mmol) of 28% aqueous ammonia was added to 1000 mL D.W. and prepared to pH 9.0 with formic acid.

Buffer-C: 100 mM aqueous acetic acid and 100 mM sodium acetate was mixed in the ratio of 14.8:35.2 and prepared to pH 5.0.

Removal of Trp, Phe and Tyr, GPR142 Possible Endogenous Ligands From Porcine Brain Extracts

The Sepabeads SP 207 elution fraction (Figure 1) was subjected to weakly acidic cation exchange chromatography. The elution fraction was loaded into the 10 mL Sigma-Aldrich Amberlite CG-50 column equilibrated with D.W. The column was washed with 40 mL of D.W. and then adsorbed components on the column were desorbed by following 80 mL of 0.1 N HCl and subject to the analysis by LC/MS to check the removal of Trp, Phe and Tyr.

Stability of the Activity in the Active Fraction

The above 0.1 N HCl eluted fraction from the weakly acidic cation exchanger Amberlite CG-50 was used for the tests.

Ten micro liters of buffer-A, D.W. or buffer-B was added to 40 μL of the eluted solution. Each sample was heated for 30 min at 60°C (Sample AH, NH or BH) or 120 min at 40°C (Sample AL, NL or BL). After heat treatment, each sample was freeze-dried once, and re-dissolved for the testing of GPR142 agonistic activity.

Molecular Size Estimation on Electrodialysis

HCl (0.1 N) eluted fraction (500 μL) from the weakly acidic cation exchanger Amberlite CG-50 (same as used for Stability Test) was electrodialyzed by using "Microacilyzer G1", a portable desalting apparatus commercialized by SUNACTIS Co., Ltd., Osaka, Japan, equipped with an AC-110 (for Mw cut 100) or AC-220 (for Mw cut 300) comprising a cation-exchange membrane and an anion-exchange membrane, both of which have a molecular weight cut-off of about 100 or 300. An amount of 0.5 M $NaNO_3$ solution (25 mL) was used as an electrode solution and final electric current was set to 0.02 A.

LC/MS-MS Analysis

LC/MS analysis was performed on an Agilent 1100 LS/MSD system. The HPLC column was a Capcellpak AQ (4.6 x 150 mm, Shiseido Co., Ltd.). Separation was accomplished with the mobile phase containing solvents A and B in gradient, where A was 0.1% heptafluorobutyric acid (HFBA) (v/v) in water and B was 0.1% HFBA (v/v) in 90% acetonitrile (v/v). The linear gradient time program was from 0% to 18% B in 15 min. The flow rate was 1.0 mL/min. The UV data were obtained with a photodiode array detector for the wavelengths from 190 nm to 400 nm and the profiles at 210 nm were extracted. A mass spectrometric detector was operated under positive ion mode and the scanned *m/z* range was from 50 to 500. The ESI interface and mass spectrometer parameters were optimized to obtain maximum sensitivity.

Results and Discussion

Characterization of an active component from porcine brain extract

Before starting the purification of an active component from porcine brain extract, heat and pH stability tests and molecular size estimation of the active component was performed.

Agonistic activity of the extract was stable both in acidic and basic conditions as well as neutral (60°C, 30 min and 40°C, 120 min, Figure 2A) and also stable at pH 1 and 13 (r.t., 2 h) (data not shown).

To exclude the possibility that the active component was a small molecule salt, desalination from the porcine brain extract sample using an electorodialyzer (microacilyzer) was performed. Electrodialysis is a technology to separate ionic substances in aqueous solution, which utilizing electrophoresis and ion exchange membranes. This technology enables efficient concentration, desalination, refining and recovery. There are two types of membranes. Anion exchange membranes allow anion permeation selectively and cation exchange membranes allow cation permeation. A large number of these membranes are placed alternately between two electrodes and apply direct current to separate ions in solution as shown in Figure 2B. Formula weight of the active component was estimated to be between 100 and 300 from the electrodialysis experiment (Figure 2C). Thus, I decided to try the basic procedures used to purify small basic compounds for the identification of the active component(s) in this porcine brain extract.

Moreover, polar basic character is inferred from ion-exchange and reversed-phase chromatographs.

- Chromatographic behavior of the agonistic activity on HPLCs

  -Reversed phase column (modified octadecyl-bonded silica [ODS] or octadecyl-bonded polymer [ODP])

  Acidic: No retention (pH 3.7, pH 5.5 and 0.04% TFA)

  Neutral: Broad elution (pH 6.4)

  Basic: No elution (pH 9.0)

-Gel filtration column (polyvinyl alcohol)

Good elution (neutral, 50 mM ammonium formate)

-Normal phase column (silica)

Good elution (CH_3CN/50 mM ammonium-formate pH 3, gradient)

In addition, high concentration of ammonium formate is necessary for good elution, but that causes high background ions in LC/MS analysis.

Identification of an Active Component From Porcine Brain Extract

The neutral amino acids L-Tryptophan (Trp) and Phenylalanine (Phe) have been reported as possible endogenous ligands from our collaboration partner Amgen. Thus, before starting to explain the identification of the active component from porcine brain extracts, I thought it necessary to confirm that the active component(s) was not either of these neutral amino acids.

The procedure for purification of the agonistic component against GPR142 from porcine brain extract samples is shown in Figure 1. Sepabeads SP 207 elution fraction (Figure 1) was subject to weak cation exchange chromatography in an acidic condition. The agonistic activity against GPR142 was eluted in the HCl fraction with a high recovery rate (EC_{50} = 5 ~ 10 μg/mL). Removal of Trp (EC_{50} = 100 μg/mL), Phe and Tyr from the eluted sample was confirmed by LC/MS analysis, thus the active component(s) was discriminated from these neutral amino acids.

LC/UV-MS profiles of the Active Fraction 1 from porcine brain extracts are shown in Figure 3. The agonistic activity against GPR142 were observed in the fraction corresponded to the peak from 9.1 min to 9.5 min as the retention time (Active Fraction 2). Several ion peaks with the peak pattern of 2 mass unit intervals were observed in the mass spectrum of Active Fr. 2 (Figure 4) throughout the retention time. The isotope peak pattern of Zn (^{64}Zn, 100%; ^{66}Zn, 57.4%; ^{67}Zn, 8.4%; ^{68}Zn, 38.7%; ^{70}Zn, 1.3%) was found to have similar 2 mass unit intervals in the MS spectrum after searching for these characteristic peak patterns of Active Fr. 2. Therefore I hypothesized that the active component in porcine brain extract may be any compound containing zinc.

Representative UV chromatograms of the reference standard $ZnCl_2$ and the Active Fr. 1 are shown in Figure 5. A similar peak was observed around 9 min, and identity of retention time and UV spectrum of both samples indicated the presence of a zinc ion in Active Fr. 1.

Thus, I hypothesized that the zinc ion may play an important role in the activation of GPR142. The activity of the reference standard $ZnCl_2$ and Active Fr. 1 were compared using IP assay in some conditions (Figure 6). $ZnCl_2$ (EC_{50} = 1.4 μg/mL [10 μM]) and Active Fr. 1 (EC_{50} = 3 μg/mL) showed almost the same efficacy against GPR142. Furthermore, these activities were both inhibited by adding EDTA.

I concluded that the active component in porcine brain was zinc ion. The preliminary results of electrodialysis experiments showed that formula weight of the active component was estimated to be between 100 and 300. However, the molecular weight of zinc is 65.38. The anionic and cationic membranes used for dialysis are essentially made from anionic and cationic exchange resins respectively. These resins have mentioned to have a typical selectivity depending on ions for analysis; e.g., the higher the charge of the ion, the stronger it interacts with the resin. For transport through a cationic or anionic exchange membrane, multivalent ions (like zinc as divalent ion) may be more strongly retained in the membrane material and thus thought to be transported more slowly(Ref. 49, 50) and retained in AC-110 (for Mw cut 100).

It is reported that Zn also acts on GPR39 (Ref. 51) and GPR83 (Ref. 52) as an endogenous agonist. The serum concentration of zinc was reported as being about 100 μg/dL (15 μM) (Ref. 53), which is enough to show biological activity against GPR142 in vivo. GPR142 is highly expressed in pancreatic beta cells and the immune system, suggesting the receptor may play the role in the control of diabetes or inflammation diseases (Ref. 54). In collaboration research with Amgen, several GPR142 agonists were discovered and they are shown to be possible insulin secretagogues (Ref. 15). At the molecular and cellular level, zinc (Zn) is known to be involved in insulin synthesis, secretion and signaling, and thus, the consequent actions

of insulin on metabolism (Ref. 55, 56). Mechanisms of GPR142 activation by zinc are still not clear, but GPR142 may play some role in insulin secretion in vivo and zinc also play an important role in insulin signaling, and the known effect of zinc to protect Type 2 diabetes may be partly from GPR142 activation.

Zinc Ion Acts on GPR142 as a Modulator, Not as an Agonist Itself

Zinc ion was found to have the agonistic activity against GPR142 in porcine brain extract. It has been reported that essential metals, Fe, Zn, Co, Ni and Mn act on OGR1 as endogenous agonists (Ref. 57). Moreover, there are some reports that metal ions such as Na^{+}, Ca^{2+}, Mg^{2+} act as allosteric modulators which activate GPCRs only with their ligands (Ref. 58, 59).

There are many reports that have suggested the modification of GPCR by Zn^{2+}. Zn^{2+} has been reported as a positive allosteric modulator of agonist binding for the β2-AR (Ref. 60). It was reported that the binding of either an agonist or an antagonist to serotonin receptor 1A (5HT1A-R) were prevented completely by zinc (Ref. 61). D1 and D2 dopamine receptors do not lose all ligand binding properties in the presence of zinc, like 5HT1A-R, but they do have decreased affinity for ligands (Ref. 62). This led me to assume that the observed GPR142 activation by zinc might be resulted from modulating the affinity of its ligand, Trp but not by direct activation of the receptor.

The zinc ions in an inositol phosphates accumulation assay (IP assay) showed agonistic activity using cultured media as an assay buffer, but not Hanks HEPES (H/H) buffer; meanwhile, Trp showed agonistic activity both with the media and H/H buffer (Figure 7). These data were consistent with my hypothesis that zinc ions act not as a ligand (agonist), but as a modulator, which changes the properties of receptor activation by both natural and surrogate ligands. It is assumed that zinc ions do not act as an agonist individually, but show agonistic activity by enhancing the agonistic activity of Trp contained in DMEM. In other words, the presence of Trp is necessary for the activity induced by zinc ions. At the same time, the enhancement of the IPs accumulation by zinc, but not by Trp was inhibited by adding EDTA, suggesting that Trp can activate GPR142 directly without the presence of zinc ions.

During the purification of zinc from porcine brain extract, I used cultured media (DMEM) as an assay buffer for the IPs accumulation testing. The composition of DMEM (Thermo Fisher Scientific, Cat. No.: 11965) is shown in Table 1. DMEM contains 78.4 μM of Trp and 400 μM of Phe, since Trp is an essential amino acid for survival. Since the EC_{50} of Trp for human GPR142 is 500 μM and that of Phe is still higher, Trp and Phe contained in the DMEM were not enough to fully activate the receptor. I hypothesized that zinc in porcine brain extract may modulate (increase) the affinity of Trp and Phe in DMEM, which induced the enhanced accumulation of secondary signal molecules.

For the further confirmation that zinc ions enhance the agonistic activity of Trp against GPR142, enhancement of IPs accumulation by zinc ions in various GPR142 agonists was tested. The reported GPR142 agonists, Trp and Phe as possible endogenous ligands and phenylalanine derivative as a synthetic small molecule agonist were used to test the enhancement of IPs accumulation by zinc ion. As shown in Figure 8, zinc modulated (increased) the affinity of not only Trp, but all of the tested compounds.

Finally, to confirm the possibility that other metal ions that may be contained in Active Fr. 2 also have agonistic activity against GPR142, I compared the effect of other metal ions on activation against GPR142 (Figure 9). Only $MnCl_2$ and $AlCl_3$ showed the same modulator activity as $ZnCl_2$, but both of them were weak compared to $ZnCl_2$. $CuSO_4$ showed agonistic activity only in Hanks/HEPES buffer but not in dose dependent manner. It may necessary to further analyze the activity of $CuSO_4$ regarding GPR142.

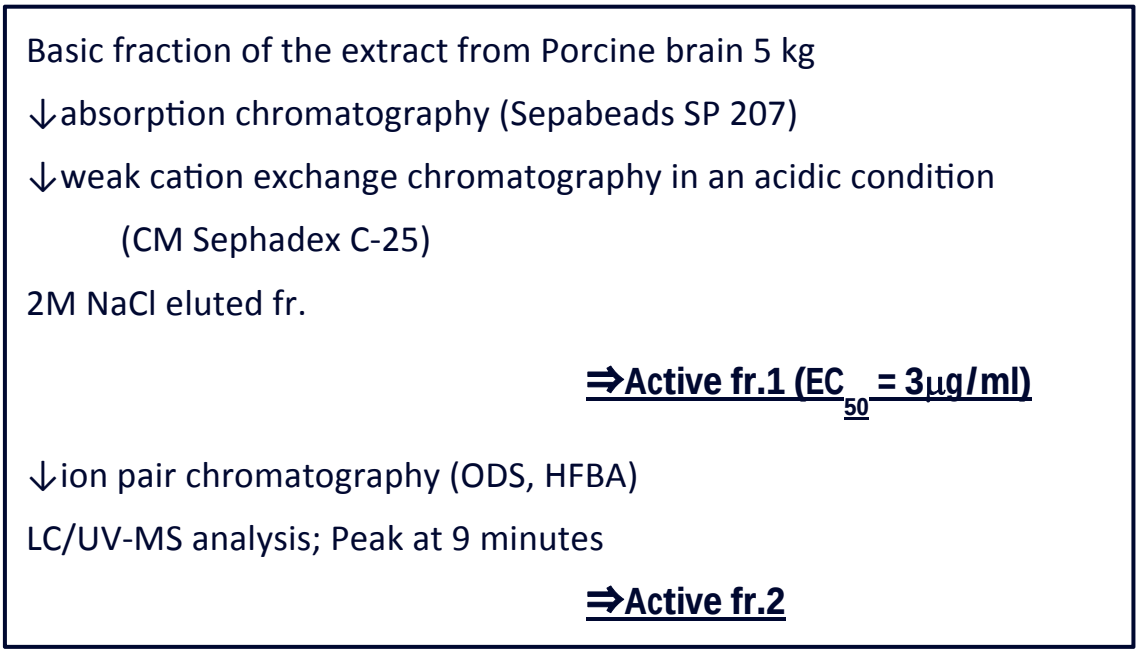

Figure 1. A schematic way of purification of the GPR142 active component(s) from porcine brain

(A)

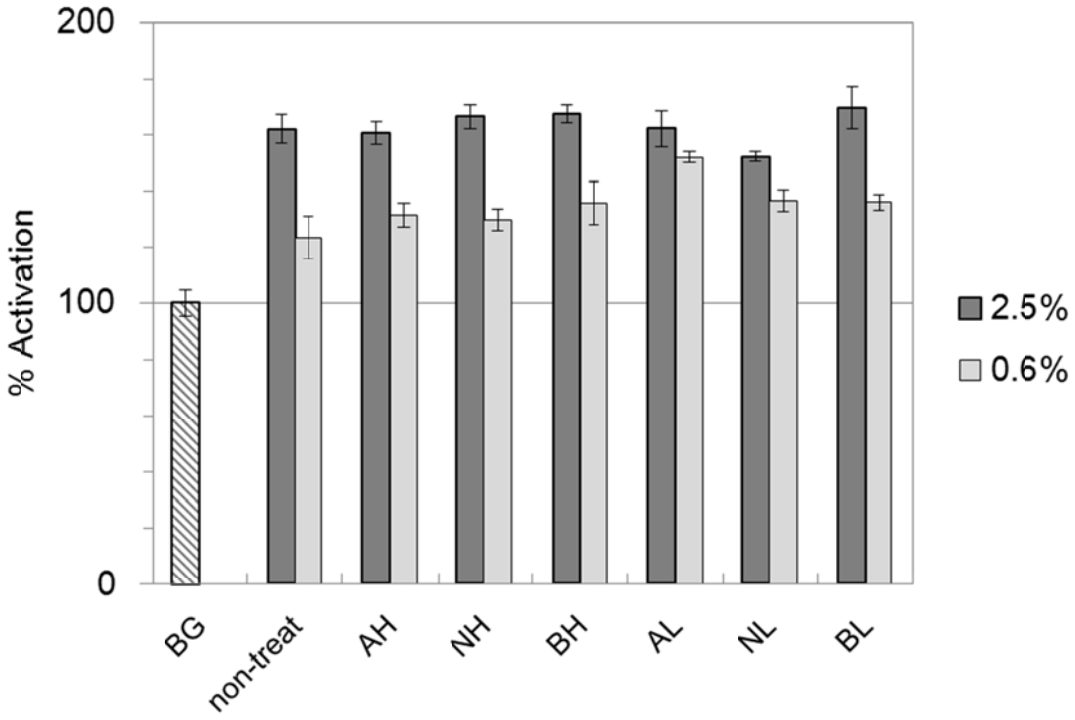

(B)

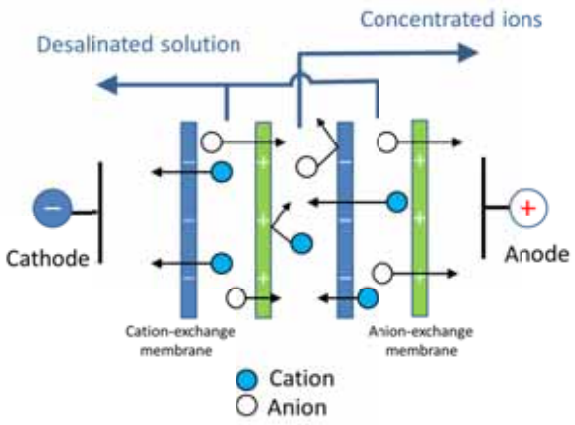

(C)

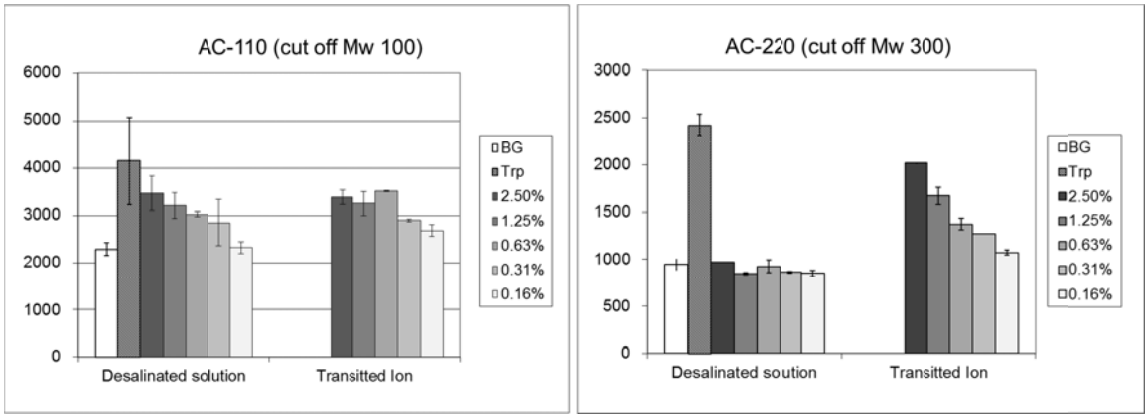

Figure 2. Characterization of an active component from porcine brain extract

(A) Stability of the active component(s). Each sample was heated for 30 min at 60°C (Samples AH, NH or BH) or 120 min at 40°C (Samples AL, NL or BL). After heat treatment, each sample was freeze-dried once, and re-dissolved for the testing of GPR142 agonistic activity at the indicated concentration (v/w). BG was negative control with D.W. and non-treat was sample freeze-dried without heat treatment. The data are presented as means of %activation from quadruplicate measurements with standard deviation shown as error bars. (B) The principle of electrodialysis. Electrodialysis (ED) is a membrane separation process that utilizes an electrical potential difference as a driving force for moving ions in solutions. (C) Molecular size estimation in electrodialysis of the active component in the fraction. After electrodialysis using a membrane that limits component molecular size to under 300 or 100, each sample was freeze-dried once, and re-dissolved for the testing of GPR142 agonistic activity at the indicated concentration (v/w).

(A)

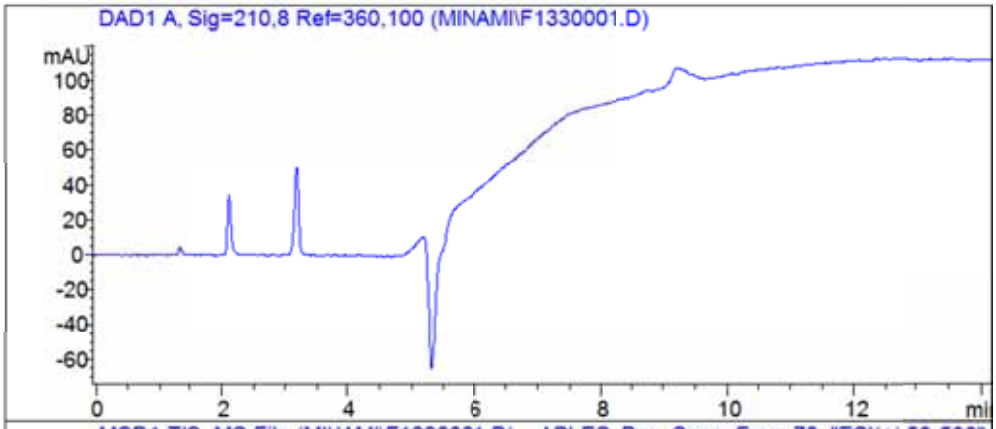
DAD1 A, Sig=210,8 Ref=360,100 (MINAMI\F1330001.D)
mAU
100
80
60
40
20
0
-20
-40
-60
0
2
4
6
8
10
12

(B)

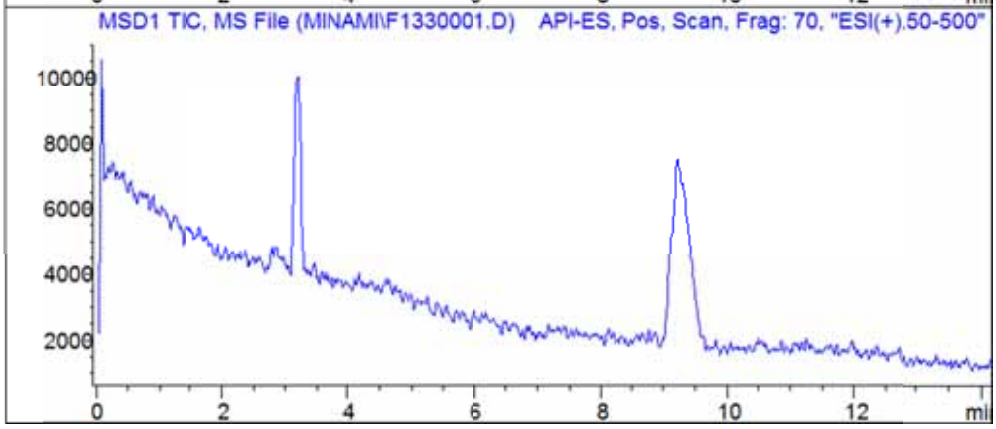
MSD1 TIC, MS File (MINAMI\F1330001.D) API-ES, Pos, Scan, Frag: 70, "ESI(+),50-500"
10000
8000
6000
4000
2000
0
2
4
6
8
10
12

(C)

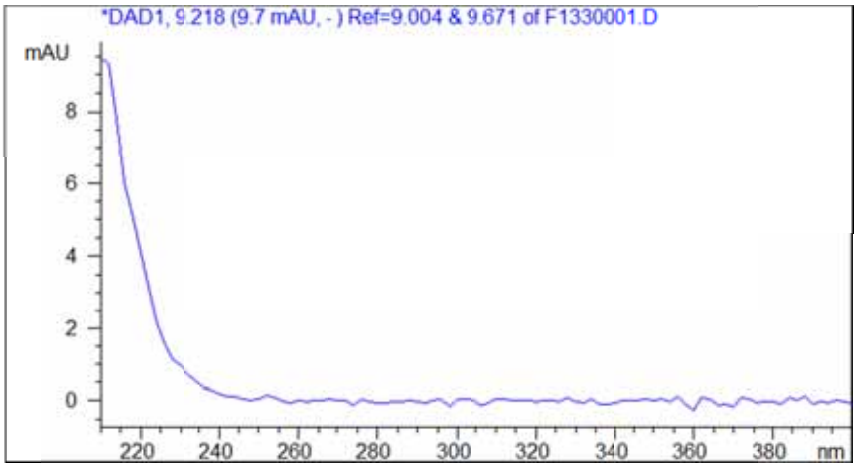
*DAD1, 9.218 (9.7 mAU, -) Ref=9.004 & 9.671 of F1330001.D
mAU
8
6
4
2
0
220
240
260
280
300
320
340
360
380
nm

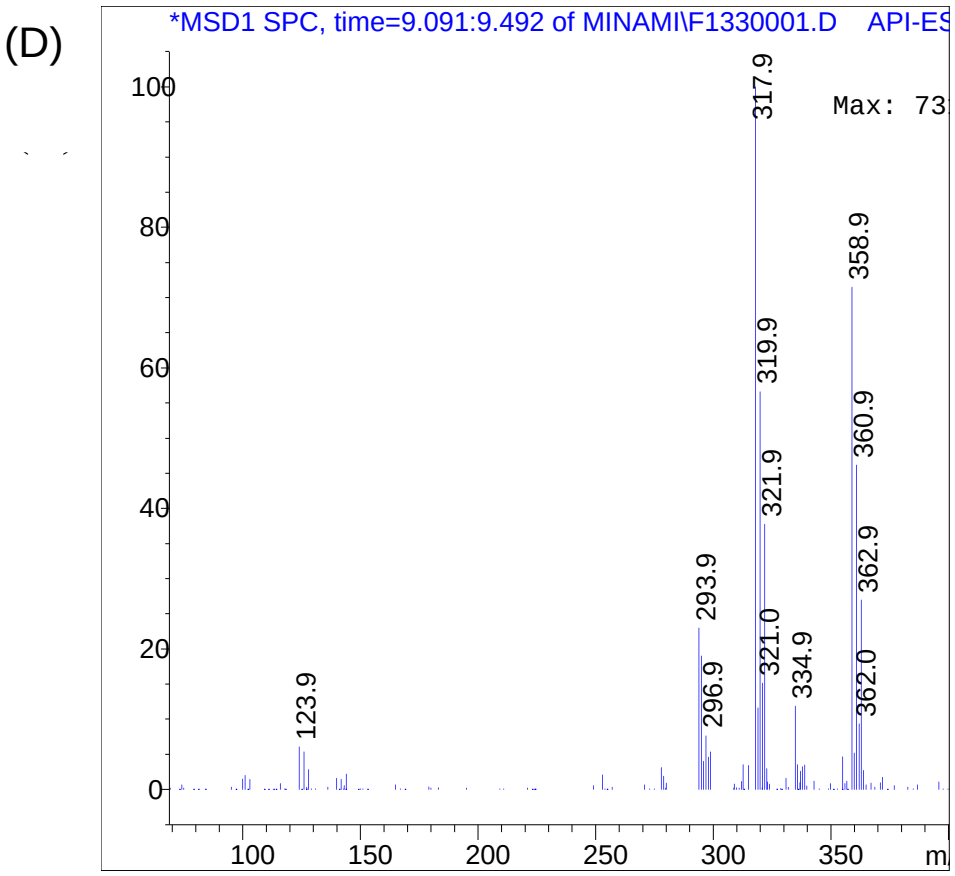

Figure 3. LC/UV-MS Profiles of the Active Fraction 1 from porcine brain extracts Column: Capcellpak AQ 4.6 x 150 mm; flow rate: 1 mL/ min; eluent: CH_3CN / H_2O - 0.1% HFBA gradient (0% -15 min - 18% CH_3CN). (A) UV chromatogram at 210 nm. (B) Total ion chromatogram (TIC) with electrospray ionization in positive ion mode; a full-scan mass spectrum covering the *m/z* range 50-500. (C) UV spectrum of Active Fr. 2 (9.2 min spectrum, as reference spectra at 9.0 min and 9.7 min). (D) MS spectrum of Active Fr. 2 (additional spectra from 9.1 min to 9.5 min, as reference spectra at 9.0 min and 9.7 min).

(A)

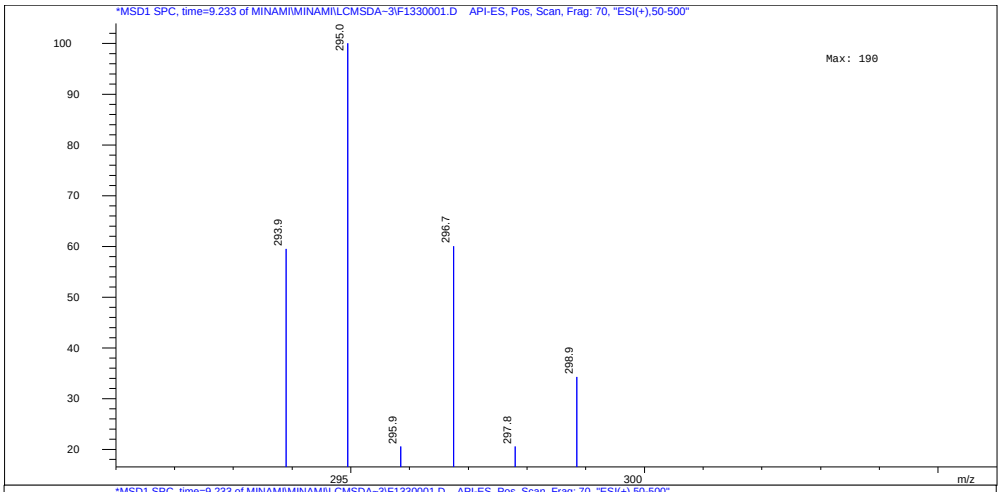
*MSD1 SPC, time=9.233 of MINAMI\MINAMI\LCMSDA~3\F1330001.D API-ES, Pos, Scan, Frag: 70, "ESI(+),50-500"
Max: 190
295.0
293.9
296.7
298.9
295.9
297.8
100
90
80
70
60
50
40
30
20
295
300
m/z

(B)

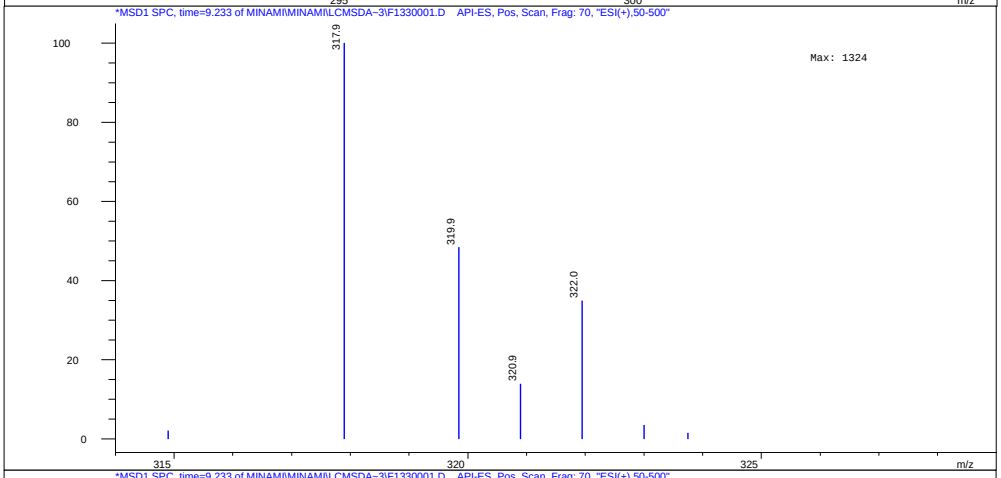
*MSD1 SPC, time=9.233 of MINAMI\MINAMI\LCMSDA~3\F1330001.D API-ES, Pos, Scan, Frag: 70, "ESI(+),50-500"
Max: 1324
317.9
319.9
322.0
320.9
100
80
60
40
20
0
315
320
325
m/z

(C)

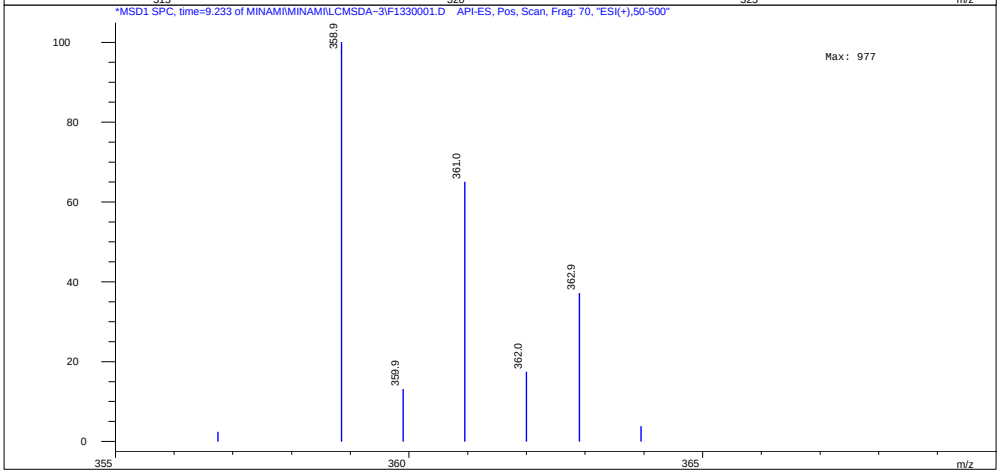
*MSD1 SPC, time=9.233 of MINAMI\MINAMI\LCMSDA~3\F1330001.D API-ES, Pos, Scan, Frag: 70, "ESI(+),50-500"
Max: 977
358.9
361.0
362.9
359.9
362.0
100
80
60
40
20
0
355
360
365
m/z

(D)

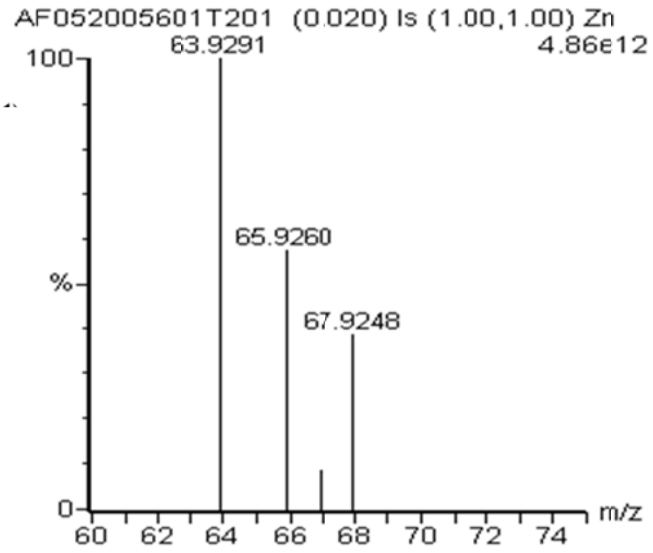

Figure 4. MS peak patterns in Active Fraction 2 from porcine brain extracts (A) ~ (C) Ion peak patterns found in the mass spectrum of Active Fraction 2. (D) Natural isotope peak pattern of Zn.

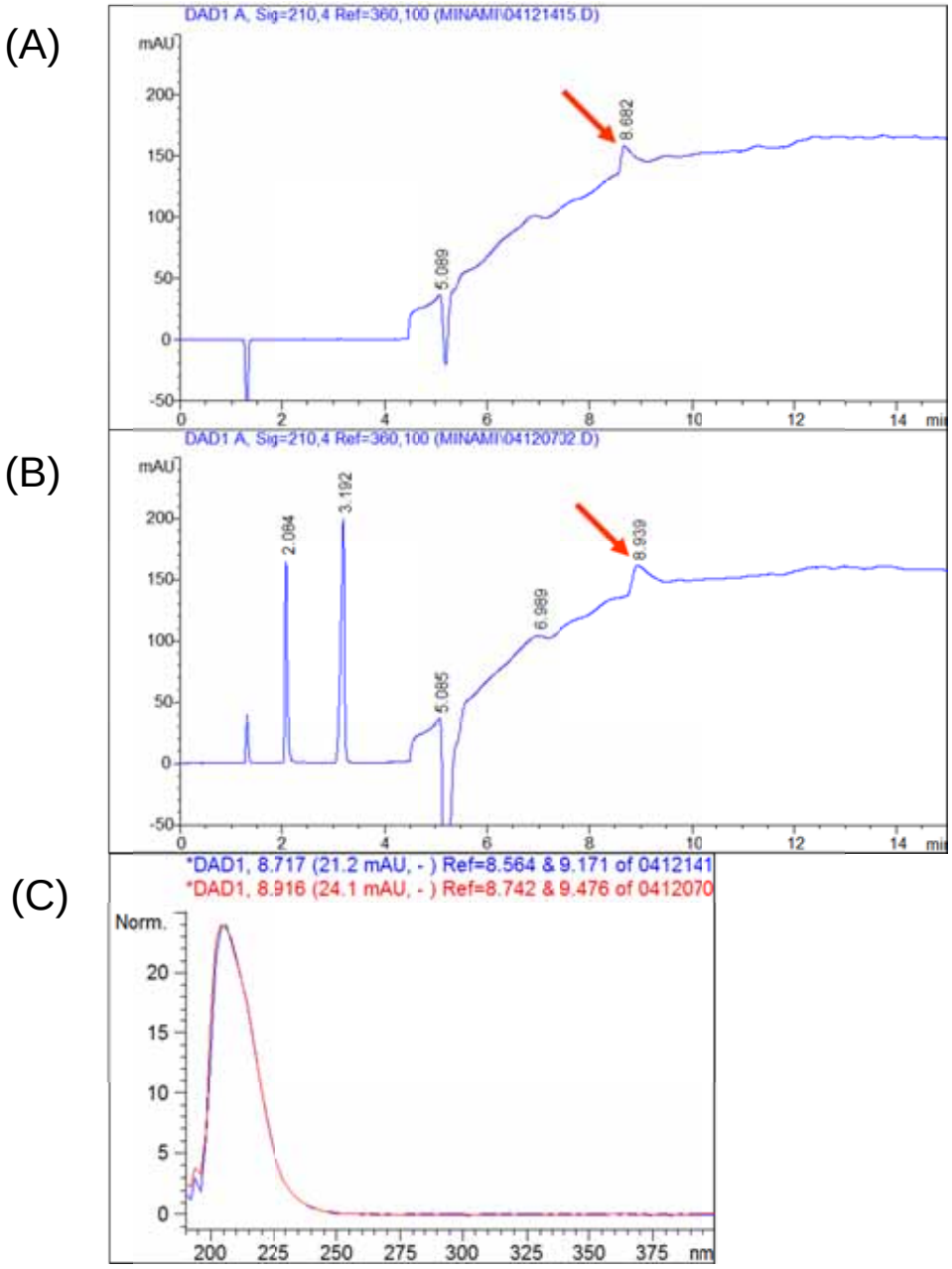

Figure 5. Comparison of standard $ZnCl_2$ and the Active Fr. 1 in ion pair chromatography

Column: Capcellpak AQ 4.6 x 150 mm; flow rate: 1 mL/ min; eluent: CH_3CN / H_2O - 0.1% HFBA gradient (0% -15 min - 18% CH_3CN); detection: UV 210 nm. (A) UV chromatogram of the standard $ZnCl_2$. (B) UV chromatogram of the Active Fr. 1. (C) UV spectra of the standard $ZnCl_2$ (blue: the spectrum at 8.7 min, as reference spectra at 8.6 min and 9.2 min) and the Active Fr. 2 (red: the spectrum at 8.9 min, as reference spectra at 8.7 min and 9.5 min).

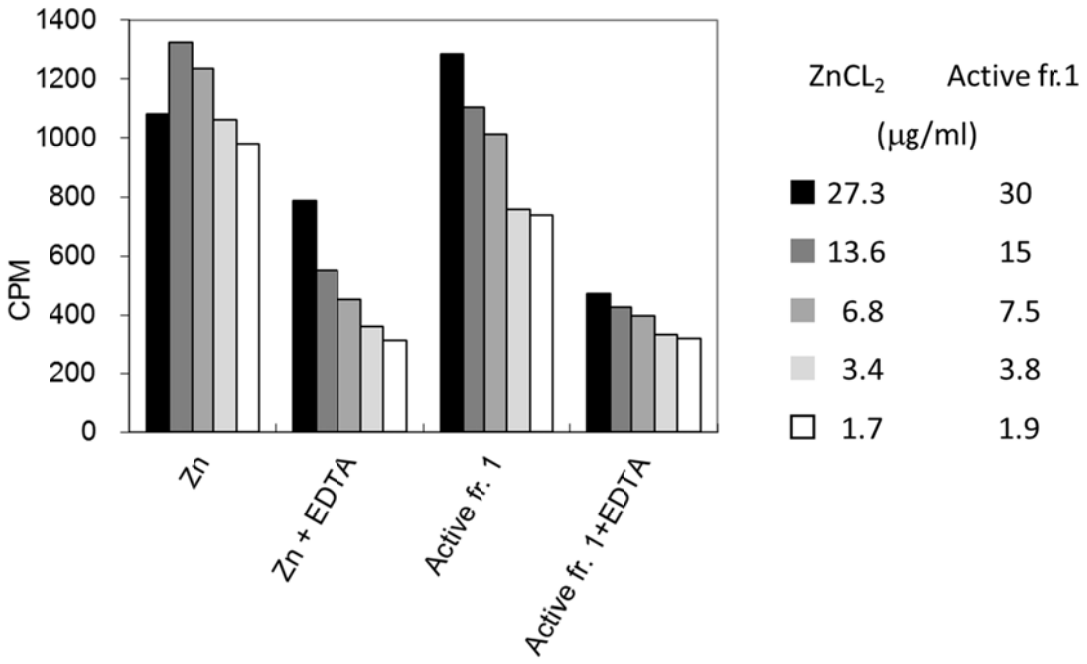

Figure 6. IP accumulation by $ZnCl_2$ and the Active Fr. 1

HEK293 cells transiently expressing human GPR142 were incubated with $ZnCl_2$ or Active Fr. 1 in the absence or presence of EDTA (1 mM) at the indicated concentrations for 90 min at 37°C. The data are presented as mean CPM value readouts from MicroBeta (Perkin Elmer).

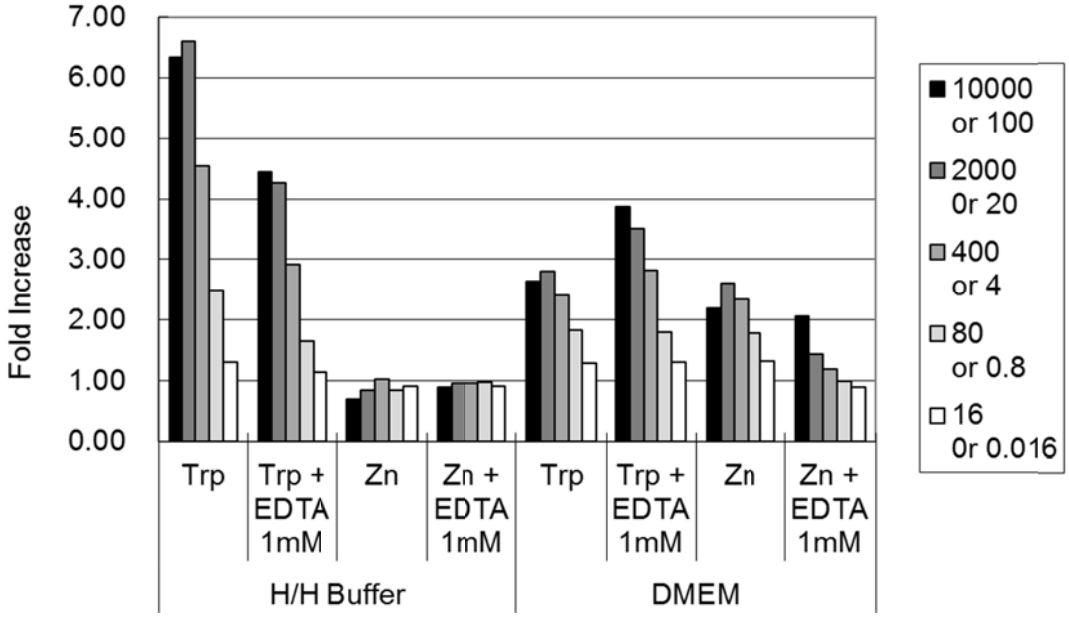

Figure 7. Zinc ion shows agonistic activity only in DMEM

HEK293 cells transiently expressing human GPR142 were incubated with Trp or $ZnCl_2$ in the absence or presence of EDTA at the indicated concentrations (μM in order) for 90 min at 37°C using H/H Buffer or cultured media (DMEM) as an assay buffer. The data are presented as mean fold increase values.

(A)

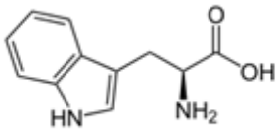

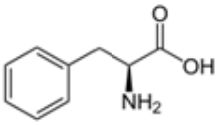

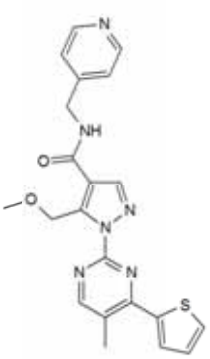

L-Tryptophan (Trp)

L-Phenylalanine (Phe)

Reported agonist pyridinone-phenylalanine scaffold (Agonist-A)

(B)

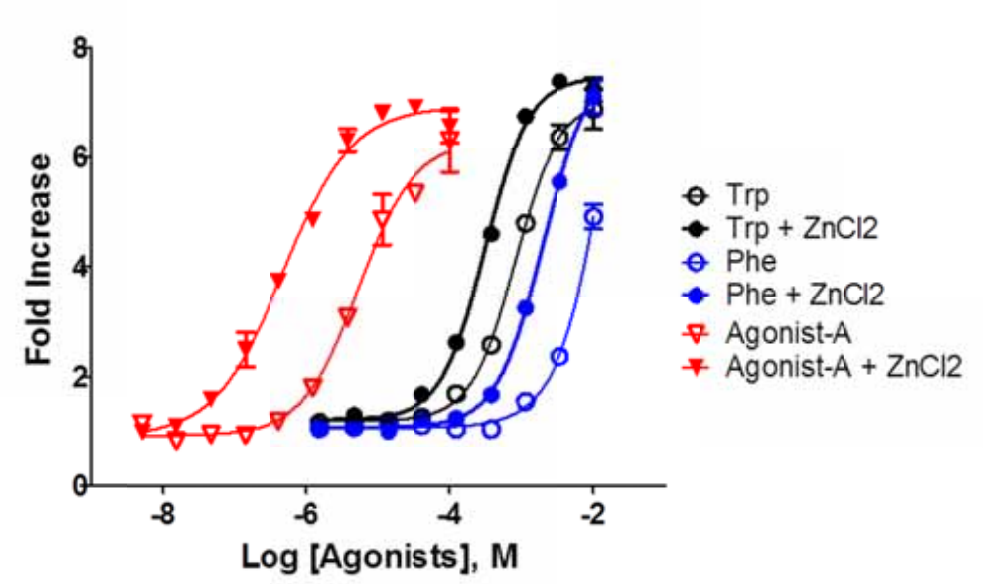

Figure 8. Enhancement of IPs accumulation by zinc ions in various GPR142 agonists

(A) Structures of the agonists tested. (B) HEK293 cells transiently expressing human GPR142 were incubated with various GPR142 agonists in the/no presence with $ZnCl_2$ for 90 min at 37°C using H/H Buffer as an assay buffer. The data are presented as mean fold increase values.

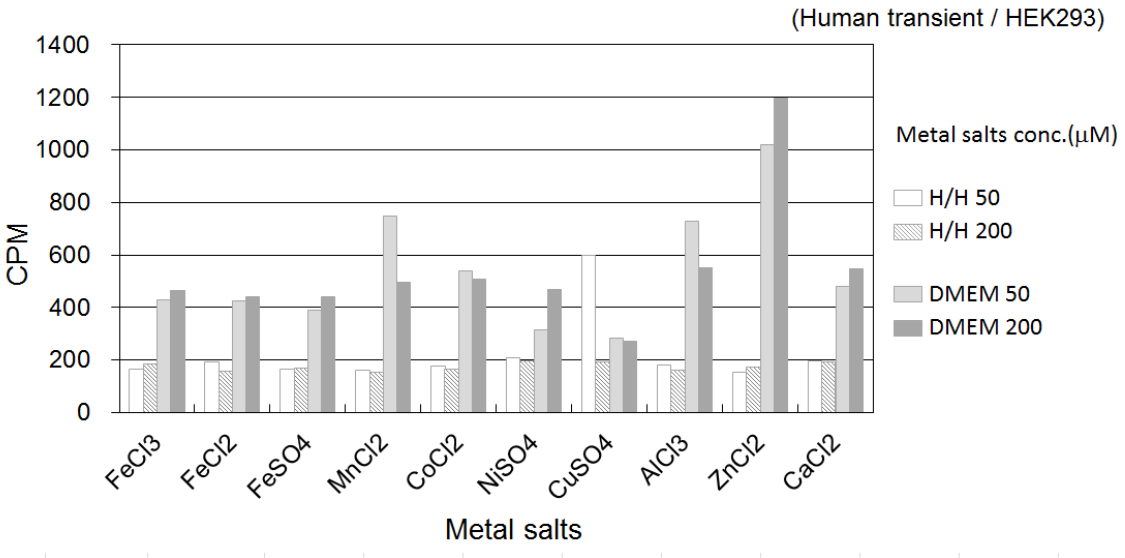

Figure 9. Enhancement of IPs accumulation of GPR142 expressing cells by various metal salts

HEK293 cells transiently expressing human GPR142 were incubated with various metal salts at the indicated concentrations (μM in order) for 90 min at 37°C using H/H Buffer or cultured media (DMEM) as an assay buffer. The data are presented as mean CPM values readouts from MicroBeta (Perkin Elmer).

Table 1. The composition of DMEM and Hanks/HEPES Buffer used as assay buffer

DMEM				Hanks HEPES buffer	
	mg/L	Mw	Conc.(M)		mg/L
$CaCl_2$	200			$CaCl_2$	140
$Fe(NO_3)/9H_2O$	0.1				
KCl	400			KCl	400
				KH_2PO_4	60
$MgSO_4$	97.67				
				$MgCl_2/6H_2O$	100
				$MgSO_4/7H_2O$	100
NaCl	6400			NaCl	8000
$NaHCO_3$	3700				
NaH_2PO_4	125				
				$NaH_2PO4/7H_2O$	90
D-Glucose	4500			D-Glucose	1000
Phenol Red	15				
HEPES	-5958			20 mM HEPES	
Pyruvic acid	-110				
Arg	84				
Cys/2HCl	63				
Gln	-584				
His HCl/H_2O	42				
Ile	105				
Leu	105				
Lys HCl	146				
Met	30				
Phe	66	165.19	4.00E-04		
Ser	42				
Thr	95				
Trp	16	204	7.84E-05		
Tyr $2Na/2H_2O$	104	181.19	5.74E-04		
Val	94				
D-Ca Pantothenate	4				
Choline Chloride	4				
Folic acid	4				
inositol	7.2				
Niacinamide	4				
Riboflavin	0.4				
Thiamine HCl	4				
Pyridoxine HCl	4				

The composition of DMEM and Hanks/Hepes Buffer were shown in Table 1. The components highlighted in grey were GPR142 active compounds.

CHAPTER 3

Discovery and Pharmacological Effects of a Novel GPR142 Antagonist

Abstract

In Chapter 2, I found an agonistic activity against GPR142 in extract of porcine brain, discriminated from L-Tryptophan (Trp) and concluded that the agonistic activity against GPR142 observed in porcine brain extract was caused by zinc ion.

GPR142 is highly expressed in pancreatic β-cells and immune cells, suggesting the receptor may play a role in the pathogenesis and development of diabetes or inflammatory diseases. In a previous scientific report (Ref. 15), our project team developed GPR142 agonists as insulin secretagogues.

In this chapter, I show the discovery of a selective, potent small-molecule GPR142 antagonist, CLP-3094, and its pharmacological characteristics. These data support targeting this receptor for the treatment of chronic inflammatory diseases.

Introduction

GPR142 is a GPCR highly expressed in the pancreas and the immune system, and shares 33% amino acid identity with GPR139 (Ref. 17). Recently, ligands for GPR139 were reported as being the essential amino acids Trp and L-Phenylalanine (Phe) (Ref. 14). GPR142 was also found to be a receptor of aromatic amino acids with Trp representing one of the most potent ligands, having an EC_{50} value of 0.2 mM to 1 mM (Ref. 15).

The high expression level of GPR142 in pancreatic β-cells suggests that the receptor may play a role in the pathogenesis and development of diabetes. In our previous research, we reported the discovery of novel GPR142 agonists as insulin secretagogues. GPR142 is highly expressed in pancreatic islets and Trp triggered glucose-stimulated insulin secretion (GSIS) in the cultured islets as well as in a rodent in vivo model dependent on GPR142 (Ref. 19). In addition, GPR142 is expressed in intestine, and Trp induced incretin secretion of glucagon-like peptide-1 (GLP-1) and glucose-dependent insulinotropic peptide (GIP) is also dependent on GPR142. Thus, our findings provide a novel mechanism for glucose homeostasis and may lead to new strategies for diabetes

treatment.

On the other hand, GPR142 is highly expressed in immune cells as well as in pancreatic β-cells. In addition, the ligands of GPR142, Trp and its metabolites, serotonin and kynurenine, are known to play important roles in inflammation (Ref. 20, 21). In order to clarify the function of GPR142 in the immune system, I used GPR142 KO mice to pursue the possibility of GPR142 as a therapeutic target for inflammation diseases. GPR142 KO mice were protected from anti-type II collagen (CII) antibody-induced arthritis, thus I hypothesized that GPR142 could be a potential target for rheumatoid arthritis (RA) treatment.

In this chapter, I present the first reporting of a pharmacological characterization of a selective, potent small-molecule GPR142 antagonist. The data provided herein supports targeting this receptor for the treatment of chronic inflammatory diseases.

Materials and Methods

Materials

An arthritogenic monoclonal antibody (mAb) cocktail was purchased from Immuno-Biological Laboratories (Gunma, Japan) and LPS was purchased from Calbiochem through Merck Millipore (Darmstadt, Germany). Bovine type II collagen (CII) was purchased from Collagen Research Center (Tokyo, Japan). Complete Freund Adjuvant (CFA) was purchased from Becton, Dickinson and Company (Franklin Lakes, NJ, USA). ELISA kits for IL-1β and TNF-α were purchased from R&D Systems. Inc. (Minneapolis, MN, USA). TRIzol reagent and TaqMan Universal PCR Master Mix, TaqMan Reverse Transcription Reagent, TaqMan Rodent GAPDH Control Reagent, and TaqMan Probes were purchased from Thermo Fisher Scientific Inc. (Waltham, MA, USA).Midazolam was purchased from Wako Pure Chemical Industries, Ltd. β-nicotinamide adenine dinucleotide phosphate sodium salt (β-NADP), and D-glucose 6-phosphate were purchased from Sigma-Aldrich (St. Louis, MO, USA). Glucose-6-phosphate dehydrogenase was purchased from Oriental Yeast Co., Ltd. (Tokyo, Japan)

All other reagents and solvents including DMSO (dimethylsulfoxide) and Tween 80 (Polyoxyethylenesorbitan Monooleate) used in this study were of either HPLC or analytical grade.

Animals

BALB/cAnNCrj (BALB/c) mice were purchased from Charles River (Tokyo, Japan). C57BL/6J Jcl mice were secured from CLEA Japan (Tokyo, Japan). GPR142-deficient mice were generated by Lexicon Pharmaceuticals, Inc. (The Woodlands, TX, USA). KO mice used for this study were backcrossed with C57BL/6 mice for at least 6 generations. All mice were purchased from the ages of 5 weeks to 6 weeks, and housed at Daiichi-Sankyo Laboratories (Tokyo, Japan), and given a standard rodent chow diet and water ad libitum. All Experimental procedures were performed in accordance with the in-house guideline of the Institutional Animal Care and Use Committee of Daiichi Sankyo.

Calcium Transient Assay (HTS format; Fluo-3)

The Calcium Transient Assay was performed as previously described (Ref. 63). Briefly, CHO-K1 stably expressing human GPR142 was plated in a 384-well microplate with 14,000 cells per well using Trp depleted DMEM supplemented with 10% dialyzed FBS and 1% Pen/Strep. 24 hours later, the media was discarded (dumped) from the cell plate and Fluo-3 AM with quencher dye with Hank's balanced salt solution (HBSS, Gibco: Thermo Fisher Scientific Inc., Waltham, MA, USA) containing 0.1% BSA (Sigma-Aldrich, St. Louis, MO, USA), 20 mM HEPES (pH 7.4) was added to the cells. The cells were then incubated for 1 h before adding the testing compounds for the screening. After 20 minutes, fluorescence intensity change was measured by adding Trp as the ligand, and by using a FLIPR TETRA (Molecular Devices, LLC., Sunnyvale, CA, USA).

Inositol Phosphate Formation Assay (HTS format; HTRF IP One Assay)

Inositol phosphate accumulation was measured using an IP-One HTRF® assay kit purchased from Cisbio K.K. The HTRF assay was performed in accordance with the manufacturer's instruction manual. Briefly, HEK293 cells were transiently transfected with human GPR142 containing plasmid using Lipofectamine 2000 reagent (Thermo Fisher Scientific Inc., Waltham, MA, USA) and plated in a culture plate on the previous day of the assay. Cells were stimulated with analytes for 90 min at 37 °C using stimulation buffer before the addition of detection reagents.

Calculations

IC_{50} and EC_{50} values were calculated using nonlinear regression curve fitting using GraphPad Prism (Graphpad Software, Inc., San Diego, CA, USA). The basal constitutive activity is expressed as a percentage of the mock transfected (pcDNA control vector) cells' activation.

Induction of Anti-Type II Collagen Antibody-Induced Arthritis (CAIA)

CAIA was induced by the method of Terato et al. (Ref. 64, 65) using an arthritogenic mAb cocktail. For the induction of arthritis, GPR142 KO or wild type (C57BL/6) littermates were injected in to the tail intravenously with 2 mg per mouse of anti-CII

antibody, and 3 days later 100 μg of LPS (Escherichia coli 0111:B4) was intraperitoneally injected. Hind paws of each mice were examined for any swelling as described previously (Ref. 66). The severity of arthritis was graded on a 0 to 3 scale as follows: 0 = normal, 1 = swelling of one digit, 2 = swelling of two or more digits and 3 = swelling of entire paw.

Induction of Collagen-Induced Arthritis (CIA)

On the day of the injection, 100 μg bovine CII was dissolved in 100 μL acetic acid (0.05 mol/L) and mixed with an equal volume of CFA until emulsified. Each of the anesthetized Female DBA1/J mice (aged 6 weeks) was immunized intradermally near the base of the tail with the emulsified solution on Day 0 and 7 or 21.

Induction of Dextran Sulfate Sodium (DSS)-Induced Colitis

Eight female C57BL/6N mice (aged 9 weeks) were randomized into a control group and DSS treated group. Colitis was induced by means of drinking water supplemented with 3% DSS (45,000–50,000 m.w.; MP Biomedicals, Santa Ana, CA), as described previously (Ref. 67). Control mice were treated in a same way with drinking water without DSS.

Treatment of Mice with CLP-3094

Twenty-four Female DBA1/J mice (aged 6 weeks) were randomized into a control group and a CLP-3094 treated group. CLP-3094 was i.p. injected into mice at a dose of 30 or 100 mg per mouse (based on its pharmacokinetic profile in this species) after LPS injection for 8 days. As a control, an equal volume of sterile vehicle (DMF/tween80/saline = 10:10:80) was injected into mice (Vehicle group).

Measurement of Blood Cytokine, L-Tryptophan and Kynurenine Levels

LPS (1 mg/kg) or anti-CII antibody cocktail (2 mg per mouse) was injected into GPR142 KO or wild type (C57BL/6J) mice intravenously. After 1 or 4 hours, respectively, venous blood was collected from anesthetized mice and centrifuged for 5 min at 13,230 *g* and supernatant was collected to obtain plasma. The concentrations of IL-1β and TNF-α in plasma were measured using ELISA kit following to the

manufacturer's instructions of each kit. The concentrations of Trp and kynurenine were measured by HPLC as previously described (Ref. 68).

GPR142 m-RNA Expression Levels in CIA Mice (RT-PCR)

Quantitative real-time PCR (RT-PCR) was performed using ABI Prism 7700 System (Thermo Fisher Scientific Inc.) to analyze the level of chemokine and cytokine mRNAs by the development of arthritis, following the manufacturer's instructions. Briefly, on Day 0 and 7 or 21, rear footpads were collected from arthritis induced mice after 5 or 7 weeks from the 1st immunization. Total RNA was extracted soon after the collections from the pooled footpads using TRIzol reagent. Using random 9-mers, 1 μg of total RNA was transcribed with TaqMan reverse transcription reagents for cDNA synthesis. TaqMan probes and primers were designed using Primer Express(Thermo Fisher Scientific Inc.), except for GAPDH. The following mouse gene-specific primers were used for amplification: GPR142 (UniGene 1847355 - Hs.574368) forward 5'-gtcttcgtcatgctctaccac-3', reverse 5'-ctgtgatgccaaagtgcagg-3'. TaqMan probes were labeled at the 3' end with the quencher dye TAMRA and at the 5' end with the reporter dye, FAM, except for GAPDH, labeled with VIC. cDNA samples were mixed with primers and TaqMan Universal PCR Master Mix as described in the manufacturer's instructions. The PCR was performed using the following parameters: 50°C for 2 min, 95°C for 10 min, and 40 cycles at 95°C for 15 s and 60°C for 1 min. RT-PCR was performed for TNF-α and IL-1ß and normalized with the GAPDH mRNA copy number from the same sample. Acquired data were analyzed using SDS Software version 1.63 (Thermo Fisher Scientific Inc.).

In vitro metabolic stability, solubility and plasma protein binding ratio of CLP-3094

In vitro metabolic stabilities were measured using rat or mouse liver S9 fractions. The residual rates of CLP-3094 and midazolam (as a positive control) were determined after incubation with liver S9 fraction (10 mg/mL) and NADPH generation systems (2.5 mM β-NADP, 10 mM MgCl2, 25 mM D-glucose 6-phosphate, and 2 units/mL of glucose-6-phosphate dehydrogenase) for 5, 15 or 30 minutes. Solubility studies were performed using JP (Japanese Pharmacopoeia)-1 (pH 1.2) or JP-2 (pH 6.8). Percent protein binding to mouse plasma was determined by the ultracentrifugation

method. The concentrations of the drug in each assays were measured using a Liquid Chromatography - tandem Mass Spectrometry (MicroMass®, Nihon Waters K.K.) (Generic method).

Pharmacokinetics study of CLP-3094

CLP-3094 was administered intravenously (0.5 mg/10 mL/kg) or orally (2.5 mg/20 mL/kg as the solution in DMSO/Tween 80/saline (10/10/80, v/v/v) or 2.5 mg/20 mL/kg as the suspension in 0.5% methylcellulose solution) to mice (male, C57BL/6J (Charles River Laboratories Japan, Inc.), 8 weeks, N=3, Fed). The blood was collected with heparin treated syringes and the plasma samples were prepared by the centrifugation for the measurement of CLP-3094 . CLP-3094 concentrations in the plasma were determined using a Liquid Chromatography - tandem Mass Spectrometry (API4000®, Thermo Fisher Scientific K.K.) (Generic method). PK parameters (total clearance (CL), distribution volume (V), area under the curve (AUCinf), maximum concentration (Cmax) and oral bioavailability (BA)) were calculated using the computer software Phoenix WinNonlin (Ver. 6.3., Certara USA, Inc.).

Results and Discussion

Induction of CAIA in GPR142 Knock Out (KO) Mice

First, as generally done, I analyzed mRNA expression levels of GPR142 in human and mouse tissues. GPR142 showed a broad expression in many tissues tested, but relatively high expression levels in the spleen and lymph nodes as well as the pancreas (data not shown). Based on the expression in immune tissues, I hypothesized that GPR142 may play a role in the control of inflammatory diseases, and planned to induce CAIA using GPR142 KO mice to analyze the potential of GPR142 as a therapeutic target.

GPR142 KO mice, both female and male, showed reduced arthritis scores and disease incidence against CAIA (Figure 10). Protection was observed using both the subjective visual score or by the objective measurement of paw swelling. This is the first report that GPR142 KO mice were resistant to CAIA induction compared to wild type mice.

Significant reduction in the severity of DSS-induced colitis in GPR142 KO mice was also confirmed by evaluation of body weight loss and colon shortening (data not shown). These data strongly suggest that GPR142 could be a potential target for treatment of inflammatory diseases.

Blood Cytokine Levels in GPR142 KO Mice Treated with LPS or Anti-CII Antibody

In order to better help understand how GPR142 is involved in the development of CAIA, I measured the levels of inflammatory cytokines, TNF-α and IL-1ß, after treatment of LPS or anti-CII antibody (Figure 11). Production of TNF-α was relatively reduced in GPR142 KO mice compared to wild type (C57BL/6) littermates in both the treated with LPS group and the treated with anti-CII antibody group; however, production of IL-1ß was reduced by LPS, but not by anti-CII antibody. These data showed the decreased production of inflammatory cytokines might partly explain how GPR142 deficiency caused the resistance to CAIA.

GPR142 Expression and Blood Trp Concentrations in Collagen-Induced Arthritis (CIA) Mice and Dextran Sulfate Sodium (DSS)-Induced Colitis Mice

I examined the mRNA expression of GPR142 in a CIA model in mice, another mouse model of rheumatoid arthritis. Mice were immunized intradermally on Day 0 and 7 or

21 with 100 μg bovine CII mixed with an equal volume of CFA until emulsified. After 5 or 7 weeks from the 1st immunization, swelling paws from the CIA mice were homogenated and GPR142 mRNA levels were quantified by real-time RT-PCR. mRNA expression of GPR142 in swelling paws from the CIA mice was relatively higher, but not significantly higher than that of vehicle treated mice (Figure 12A). At the same time points of the experiment, the GPR142 natural ligand, Trp, concentrations in sera from the CIA mice were reduced and its metabolites, collectively called kynurenines, and known as inflammatory mediators, were increased (Figure 12B). Similar tendencies were observed in DSS-induced colitis mice (Figure 13). These results suggested there being an increased degradation of Trp in CIA and DSS colitis mice.

Furthermore, Trp degradation was observed as being lower in GPR142 KO mice than in wild type mice (Figure 14).

Establishment of Biochemical Assays for the Screening of GPR142 Antagonist

For the GPR142 antagonist screening campaign, I first established the 384-well plate calcium transient assay. Changing to the culture media using Trp depleted DMEM and dialyzed FBS the night before the assay was essential to obtaining a sufficient GPR142 signal since DMEM contains 78.4 μM of Trp and 400 μM of Phe and these amino acids activate the receptor weakly but continuously, which leads to the de-sensitization of the receptor. Overnight depletion of Trp is needed to recover the receptor fully from de-sensitization.

To evaluate the quality of the calcium transient assay, the Z' factor value was calculated using the following equation (Ref. 69).

$$Z' \text{ factor} = 1-(3\sigma_{high} + 3\sigma_{low})/(Av_{high}-Av_{low})$$

SD: Standard Deviation, Av: Average

high: High control, low: Low control

The Z' factor is a general tool for the validation and evaluation of any bioassay in general and in particular, for assays for High Throughput Screening(HTS). The Z' factor value for the calcium transient assay for human GPR142 antagonist screening from data of Figure 15 was 0.63 with limited numbers (n = 16) of positive (high, 1 mM Trp) and negative (low, no Trp) controls. In general, It is considered that when the Z' value is greater than 0.50, the assay is considered to be of high quality and to be suitable for HTS.

Next, I setup the 384-well plate IP-One HTRF® assay for GPR142 antagonist screening. In Chapter 2, I used radio-labeled ^{3}H-myo-inositol to measure the inositol phosphate accumulation subsequent to the activation of the receptor. But this protocol was complicated and expensive, and moreover the usage of radio-labeled materials for the screening was troublesome. The IP-One HTRF® assay described here offers a simple, sensitive, cost-effective, and homogeneous screening method for seeking GPR142 antagonists. Another advantage of inositol phosphate accumulation measurement is that this method is generally thought to be more sensitive compared to the calcium transient assay. The calcium transient assay can quickly measure (transient) activation of the receptor within a few minutes (usually 1-3 minutes), on the other hand the IP-One HTRF® assay measures the accumulation of inositol phosphates within 90 minutes in accordance with the increase of intercellular calcium concentration. Very weak, undetectable levels of increase in intercellular calcium ions can cause (trigger) inositol phosphate formation, and the accumulation can be detectable with a relatively long time period.

Identification of CLP-3094, a GPR142 Specific Antagonist

Through a high throughput screening (HTS) campaign, I identified several GPR142 antagonists with moderate potency, including Serotonin (5-HT1D) selective agonist, NOT (5-(nonyloxy)tryptamine) (Figure 16A). Serotonin is one of the structurally related metabolites of Trp. Serotonin itself did not have any effect on GPR142, neither did any other serotonin agonists or antagonists tested, except for NOT. Antagonist activity of NOT was relatively weak, the IC_{50} value was 3 μM against 200 μM Trp for the mouse receptor (data not shown).

The compound of greatest potential obtained was CLP-3094, a benzimidazol class of compound (Figure 16B). CLP-3094 inhibited both an increase of intracellular Ca^{2+} concentration ($[Ca^{2+}]_i$) induced by Trp using CHO-K1 cells expressing GPR142 in the aequorin assay, and an accumulation of inositol phosphates using HEK293 cells expressing GPR142 in a SPA assay. The IC_{50} value of CLP-3094 was 0.2 μM (Table 2) against 200 μM Trp for the mouse receptor and 2.3 μM against 1 mM Trp for the human receptor in the aequorin assay. CLP-3094 also inhibited the insulin secretion from islets induced by both Trp and GPR142 agonists (data not shown). CLP-3094

demonstrated itself to be a highly GPR142 specific antagonist, showing no inhibitory activity either for the serotonin receptor or the other tested GPCRs (Ghrelin, CCR4, CCK1), but showed itself to have about a 10 times weaker, partial antagonistic activity (~30% maximum inhibition) against the closely related GPCR, GPR139 (Table 2).

CLP-3094 Worked Also as an Inverse Agonist

Heterologous expressions of GPCRs have sometimes been result in the induction of ligand-independent signal in an essentially linear fashion with increasing levels of GPCR expression (Ref. 70). Milligan et al. demonstrated that the constitutive activity of GPCR was not associated with the presence of endogenous agonists, and many traditional 'antagonists' were shown to have the ability to block these constitutive activity of expressing GPCRs. These compounds have been reclassified as inverse agonists (Ref. 71).

Overexpression of mouse GPR142 in HEK293 cells led to an increase in inositol phosphate accumulation, compared to mock transfected cells (Figure 17). However, human GPR142 showed the same level of inositol phosphate accumulation as the control mock transfected in HBSS containing 20 mM HEPES and 0.1% BSA (H/H buffer), suggesting high constitutive activity in mouse receptors, but not in human ones. CLP-3094 inhibited this constitutive activity of mouse GPR142 (in H/H buffer), but showed no inhibition against human GPR142, which suggested it's being in a basal state. On the other hand, when using cultured media (DMEM + 10% FBS) as an assay buffer, human GPR142 also showed the increase of accumulation caused by Trp and Phe contained in DMEM and in serum. Though the reported serum concentration of Trp was about 13 μg/mL (65 μM) (Ref. 72), which is not enough to show full biological activity against GPR142 in vivo, GPR142 may be constitutively activated in vivo, and CLP-3094 could inhibit both mouse and human GPR142 to the basal levels.

These data suggest that CLP-3094 worked not only as an antagonist, but also as an inverse agonist against GPR142. This inverse agonist profile of CLP-3094 was also confirmed in an NFAT Luciferase assay (data not shown).

Effect of CLP-3094 on CAIA Mice

Next, to assess the therapeutic potential of GPR142 inhibition by CLP-3094, I

assessed the efficacy of CLP-3094 in the CAIA mouse model. Mice were i.v. administered 2 mg of anti-collagen antibody, followed by i.p. administration of 50 μg of LPS. CLP-3094 was i.p. administered at doses of 30 or 100 mg/kg daily from Day 0 to Day 11. Swelling of the paws was examined daily after LPS injection. Disease severity was assessed periodically, and clinical signs of disease were scored.

The severity of arthritis was scored and plotted as shown in Figure 18. The results showed that administration of CLP-3094 dose-dependently reduced, by not much, the arthritis scores. CLP-3094-treated mice consistently displayed significantly lower severity of arthritis scores than vehicle treated mice ($p = 0.03$ by repeated measures 1-way ANCOVA test).

Pharmacokinetics of CLP-3094

The results of in vitro metabolic stability study, solubility study and protein binding study were shown in Table 3. CLP-3094 was much less stable than midazolam after the incubation with rat or mice liver S9 fraction. CLP-3094 showed high solubility in JP-1 but not in JP-2. The plasma protein binding ratio of CLP-3094 was very high (over 99%) and therefore it means that the free fraction of this compound in the plasma is very low (less than 1% of the plasma concentration).

The mouse PK profiles and PK parameters after intravenous or oral administration of CLP-3094 were determined and shown in Fig. 19 and Table 4. Total clearance (CL) , distribution volume (Vd) and t1/2 in the plasma of this compound were 48.9±6.9 mL/min/kg, 0.981±0.261 L/kg and 0.740±0.363 h, respectively. The oral bioavailability (BA) of solution or suspension was 35.5±43.5% or 6.35±1.36%, respectively.

To elucidate the physiological function of GPR142 especially in immune systems, I aimed to identify selective compounds for GPR142. Through an HTS campaign using an aequorin assay, I identified a GPR142 selective antagonist with moderate potency, CLP-3094. The administration of CLP-3094 dose-dependently reduced the arthritis scores, but not by much. One of the reasons explaining this insufficient effect of CLP-3094 on inhibition of CAIA could be the in vivo rapid clearance of CLP-3094 itself ($T_{1/2}$ = 1.71 h). Since the IC_{50} of CLP-3094 is sub-micromolar, an efficacious concentration may not be maintained well enough to show a sufficient inhibition. The PK profiles of CLP-3094 might be able to explain its insufficient in vivo efficacy.

There is also a concern that the effect of CLP-3094 on CAIA is produced not only through GPR142, but partially via the closely related GPCR, GPR139, since CLP-3094 had weak antagonistic activity against GPR139 in the in vitro aequorin assay. Both GPR142 and GPR139 share the same ligands, the essential amino acids Trp and Phe. But GPR139 is exclusively expressed in the central nervous system (CNS) (Ref. 16, 17) and in situ hybridization experiments in mouse brain showed that GPR139 mRNA is abundantly expressed in the septum, caudate, habenula, zona incerta, and medial mammillary nucleus. In addition, Trp and its metabolites, serotonin, and kynurenine, are widely known to play an important role in CNS disease (Ref. 73, 74). It is considerable that GPR139 is mainly expressed in CNS and plays specific roles in the modulation of brain functions, while on the other hand, GPR142 is mainly expressed in immune cells and in the controlling of inflammatory diseases, with the exception being its expression in pancreatic β-cells. There are two reports on discoveries of GPR139 antagonists (Ref. 75, 76), but the pharmacological functions of these antagonists have not yet been reported. I am anticipating this future research.

The CAIA model is an excellent system for studying human rheumatoid arthritis, as it requires only a few weeks to receive the results (Table 5). The modulation of pro-inflammatory cytokines, such as TNF-α, IL-1ß and IL-12, using either small molecule inhibitors or biologics is crucial to control rheumatoid arthritis, and many trials are still in progress to demonstrate this concept (Ref. 77-79). CAIA requires immune complex formation and complement activation, but induction of arthritis in this model is B cell and T cell independent and does therefore not recapitulate the complexity of immune and tissue remodeling responses during human rheumatoid

arthritis (Ref. 80). The reduced sensitivity of GPR142 KO mice to CAIA suggested that involvement of GPR142 in development of arthritis is B cell and T cell independent.

I also used another mouse arthritis model, CIA, for the further analysis of the function of GPR142. The messenger RNA expression level of GPR142 was higher in CIA mice compared to control CFA mice. At the same time point of the disease, Trp degradation increased. A similar tendency was observed in DSS-induced colitis, a model of human Crohn's disease. The DSS-induced colitis model is a little more complicated. Inflammatory bowel disease is characterized by sustained intestinal mucosa inflammation, which is mainly caused by excessive macrophage activation and Th1 and/or Th17 immune responses. Oral DSS activates intestinal macrophages, leading to massive production of inflammatory cytokines and chemokines. Subsequently, a number of lymphocytes are recruited to the inflamed sites, resulting in Th1 and Th17 responses.

The degradation of Trp generates neuroactive metabolites, kynurenines, and the kynurenine pathway is under the tight control of inflammatory mediators (Ref. 73). It is a well-known mechanism that GPCRs become desensitized when exposed to their ligand for a prolonged period of time (Ref. 81). The hypothesis that increased production of inflammatory cytokines might accelerate the degradation of Trp, which decreases the desensitization of GPR142, corresponds reasonably well with the experimental data. But, further examination of GPR142 remains before truly understanding how GPR142 is involved in the development of CAIA or CIA, as well as DSS colitis.

In a previous paper, we reported the development of novel GPR142 agonists as potent insulin secretagogues. In this chapter, I showed that a GPR142 antagonist reduced the severity of CAIA in a mouse model, suggesting the receptor also may play a role in the immune system. To develop GPR142 agonists or antagonists as clinical drugs, I should work in a more determined way to clarify how GPR142 is involved in inflammatory diseases; and I will always need to follow both concurrently, from the standpoint of assessing side-effects dependent upon the relationship between agonists and antagonists.

Acknowledgments

This chapter is derived in part from an article published in Journal of Receptors and Signal Transduction, published online: 03 Nov 2016, copyright Taylor & Francis, available online: http://www.tandfonline.com/, http://dx.doi.org/10.1080/10799893.2016.1247861.

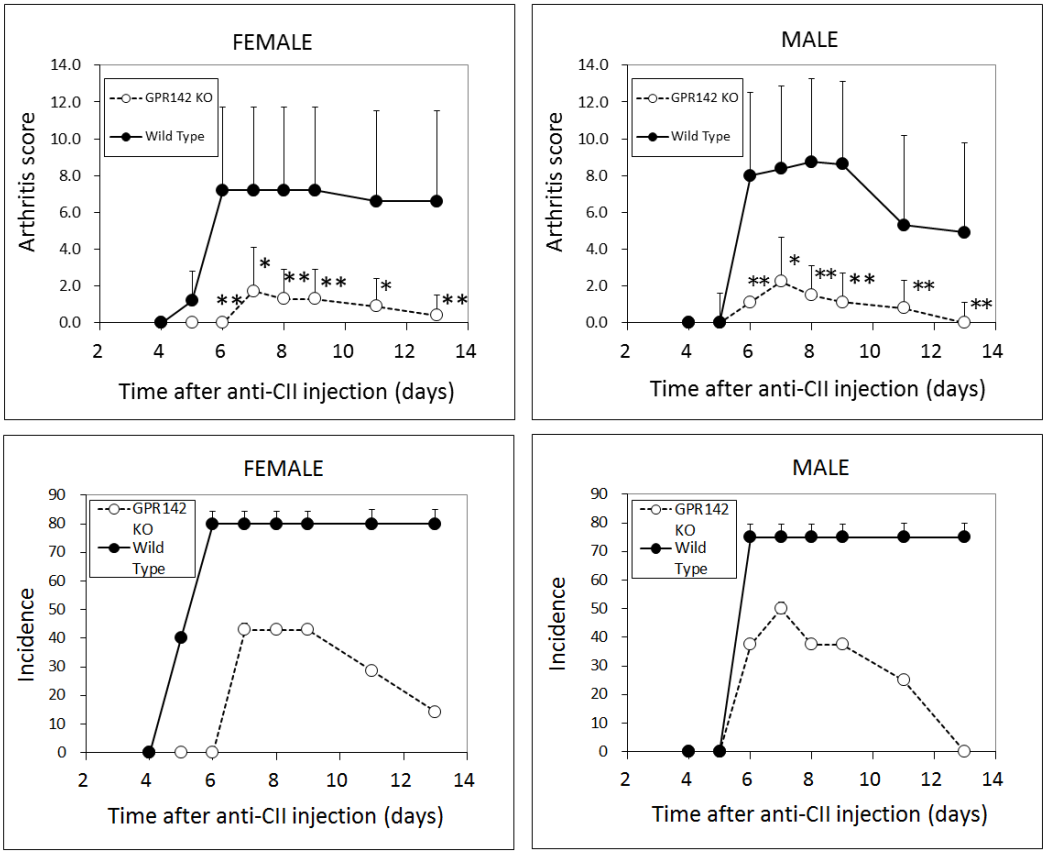

Figure 10. GPR142 deficiency reduces sensitivity to CAIA in mice

Wild type group (n = 5) and GPR142 knock out group (n = 8), 10-week old mice were treated via i.v. on Day 0 with 2 mg anti-CII antibody and subsequently boosted with 100 μg of LPS on Day 3 to induce collagen induced antibody arthritis. Arthritis score (A) and incidence (B) are shown as mean (S.E.M.) in different groups of GPR142 knock out and wild type (C57Bl/6) littermates. Closed circle: GPR142+/+ (Wild type) mice; Open circle: GPR142–/– (GPR142 KO) mice. *P < 0.05, **P < 0.001

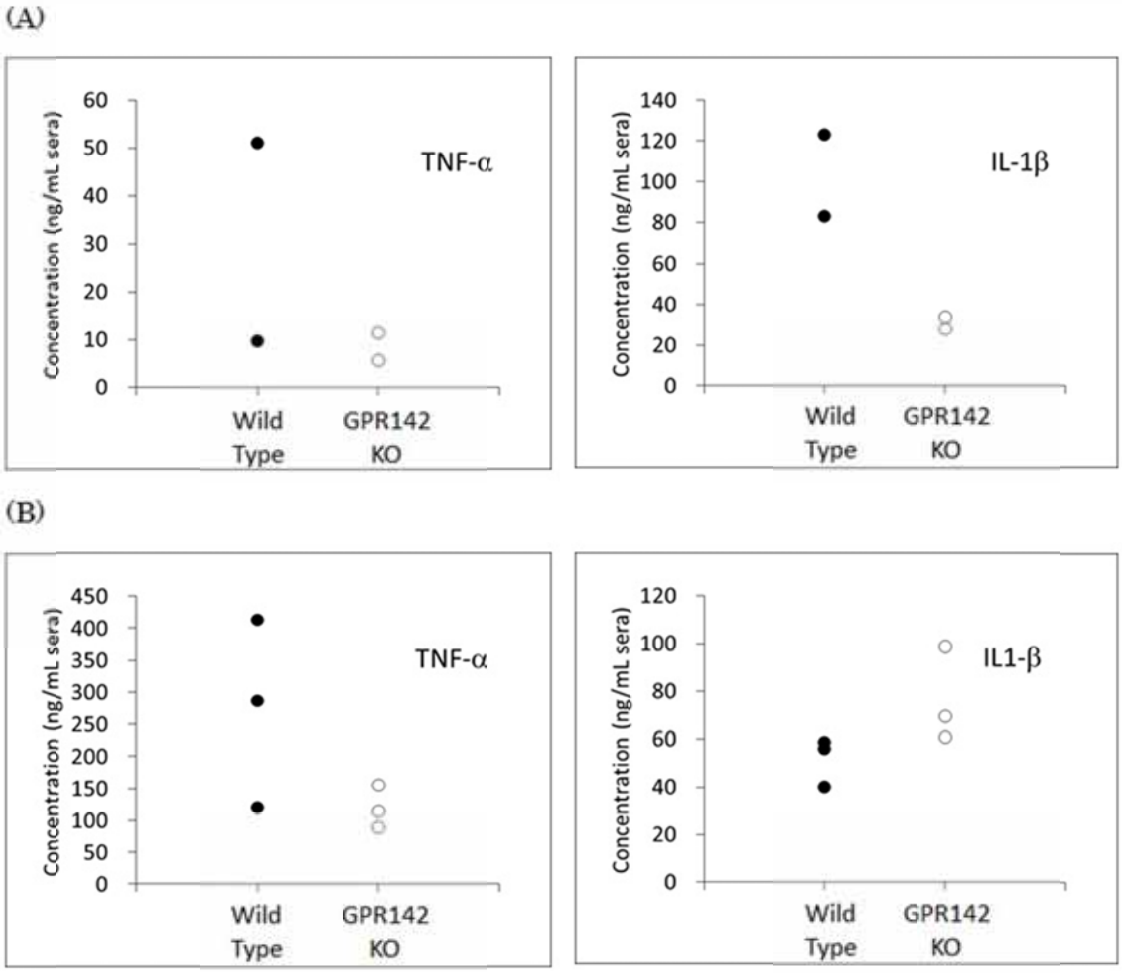

Figure 11. Blood cytokine levels in GPR142 KO mice treated with anti-type II collagen antibody or LPS

LPS (1 mg/kg) or anti-type II collagen antibody cocktail (anti-CII) (2 mg per mouse) was injected into Wild type C57BL/6J or GPR142 KO, male 14-week old mice intravenously. The serum concentrations of each cytokine were measured as described in *Materials and Methods*.

The concentration of each cytokine was plotted 1 hour after treatment with LPS (A) and 4 hours after treatment with anti-CII (B).

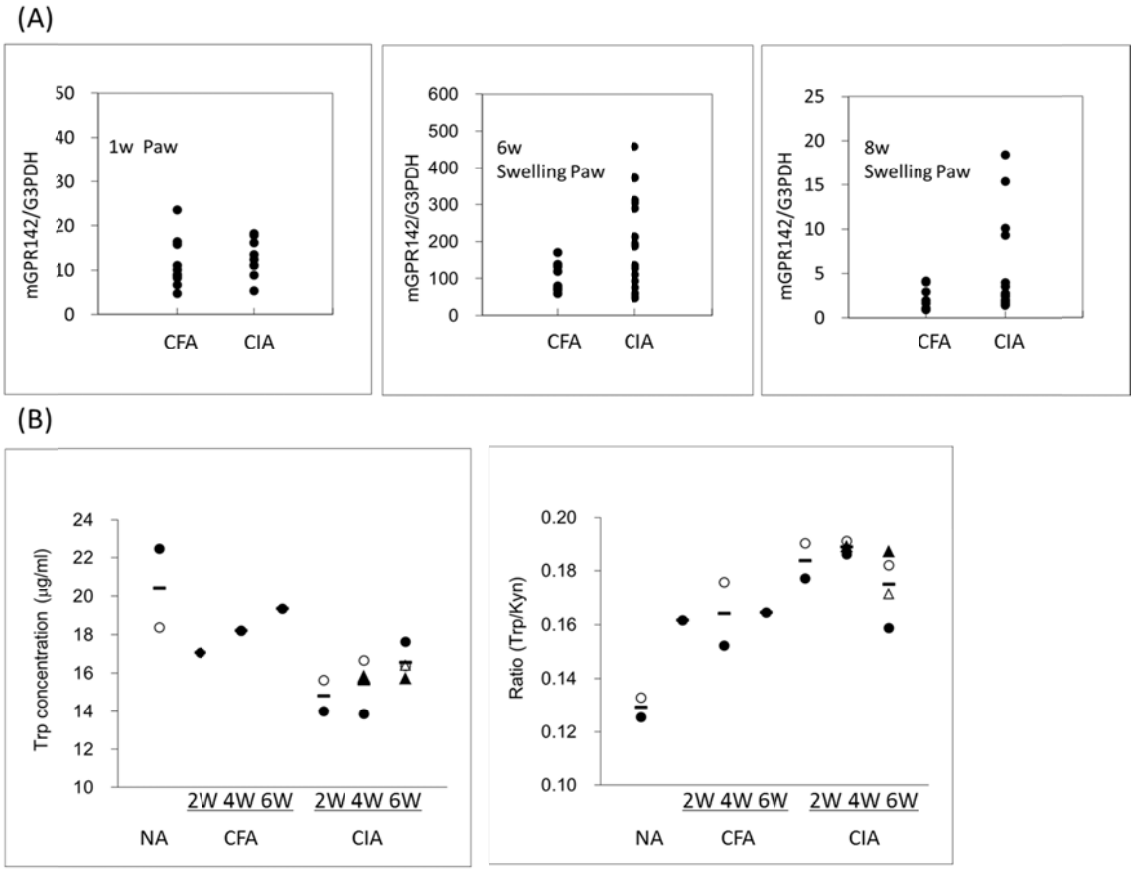

Figure 12. GPR142 m-RNA expression and L-Tryptophan levels in CIA mice

Female DBA1/J mice (6 weeks old) were immunized intradermally on Day 0 and 7 or 21 with 100 μg bovine CII dissolved in 100 μL acetic acid (0.05 mol/L) and mixed with an equal volume of CFA until emulsified. The internal control group of mice received an equal volume of CFA without CII.

(A) GPR142 mRNA levels in swelling paw from CIA and control mice were quantified by RT-PCR soon after, after 5 weeks from, or after 7 weeks from the 1st immunization. The Y-axis indicates the treatment of mice. CFA stands for CFA treated control mice without CII, and CIA stands for CIA induced mice treated with CFA and CII.

(B) The serum concentration of Trp and its metabolite, kynurenine, were measured as described in *Materials and Methods*. The concentration of Trp and ratio of Trp to kynurenine was plotted. The Y-axis indicates the treatment of mice. N stands for normal, CFA stands for mice treated only with CFA, and CIA for CIA induced mice treated with both CFA and CII. Each symbol stands for the data from the same mice. Bar shows the average value for the same conditions.

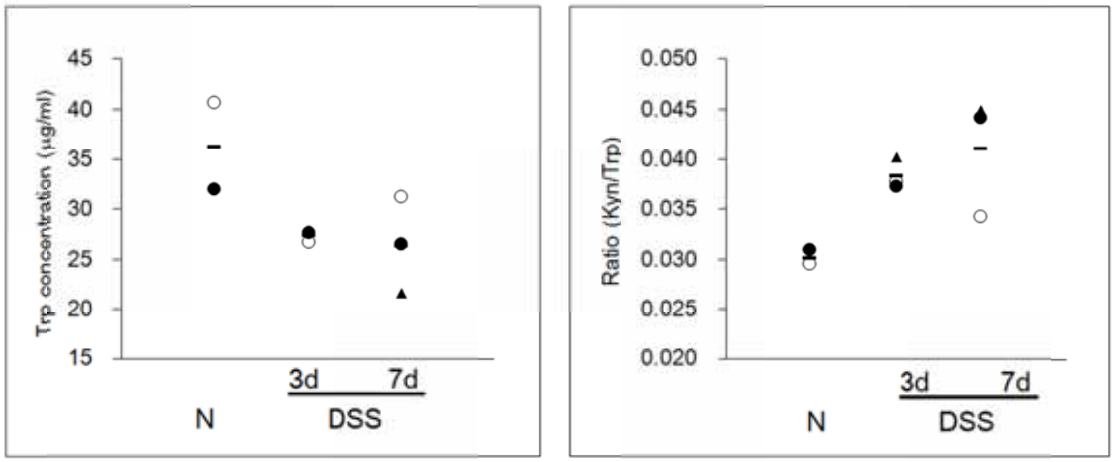

Figure 13. L-Tryptophan levels in DSS-induced colitis mice

The serum concentration of Trp and its metabolite, kynurenine, were measured as described in Materials and Methods. The concentration of Trp and ratio of Trp to kynurenine was plotted. The Y-axis indicates the treatment of mice. N stands for normal, DSS stands for mice treated with DSS, number-d stands for the day after DSS treatment. Each symbol stands for the data from the same mice. Bar shows the average value for the same conditions.

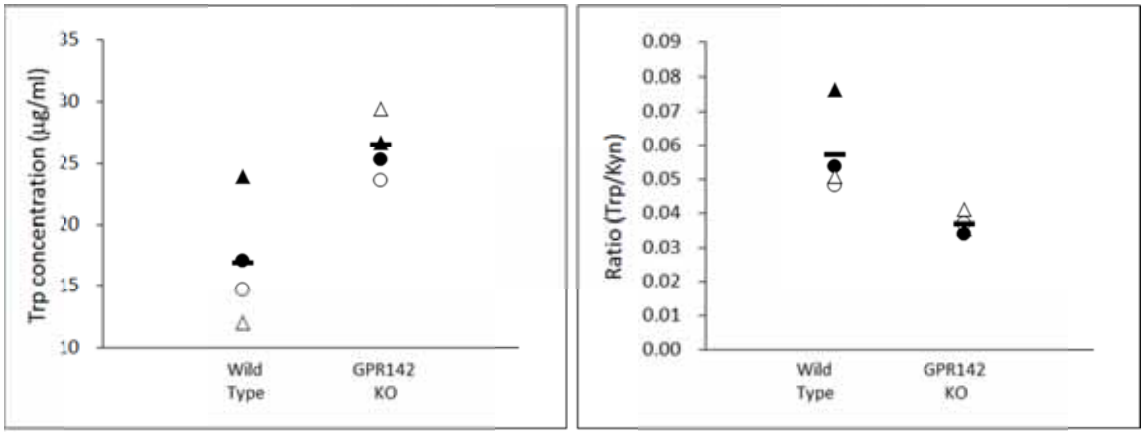

Figure 14. Blood L-Tryptophan levels in GPR142 KO mice

The serum concentrations of Trp and its metabolite, kynurenine, in wild type C57BL/6J or GPR142 KO, male 10-week old mice were measured as described in *Materials and Methods*. The concentration of Trp and ratio of Trp to kynurenine was plotted. Each symbol stands for the data from the same mice.

(A)

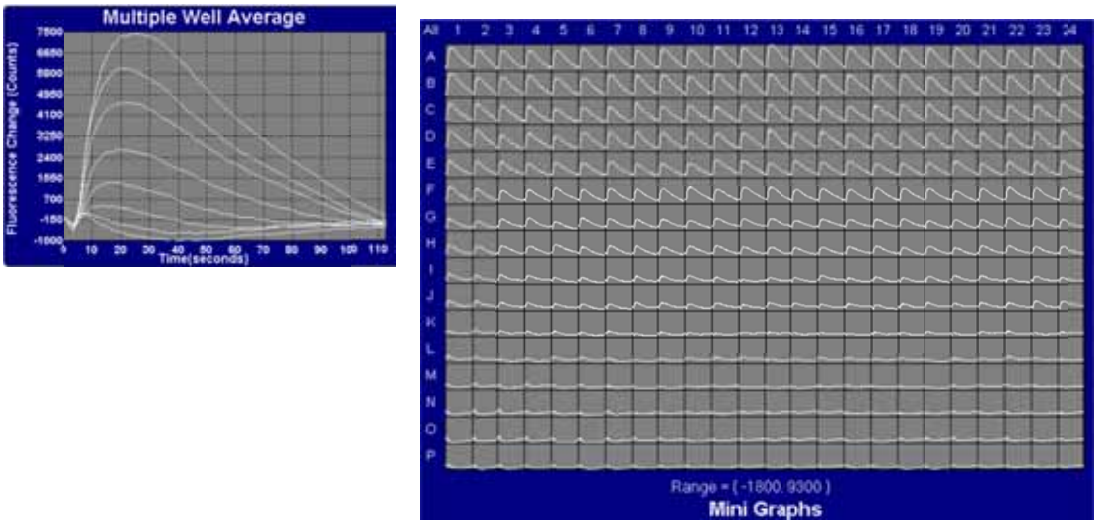

(B)

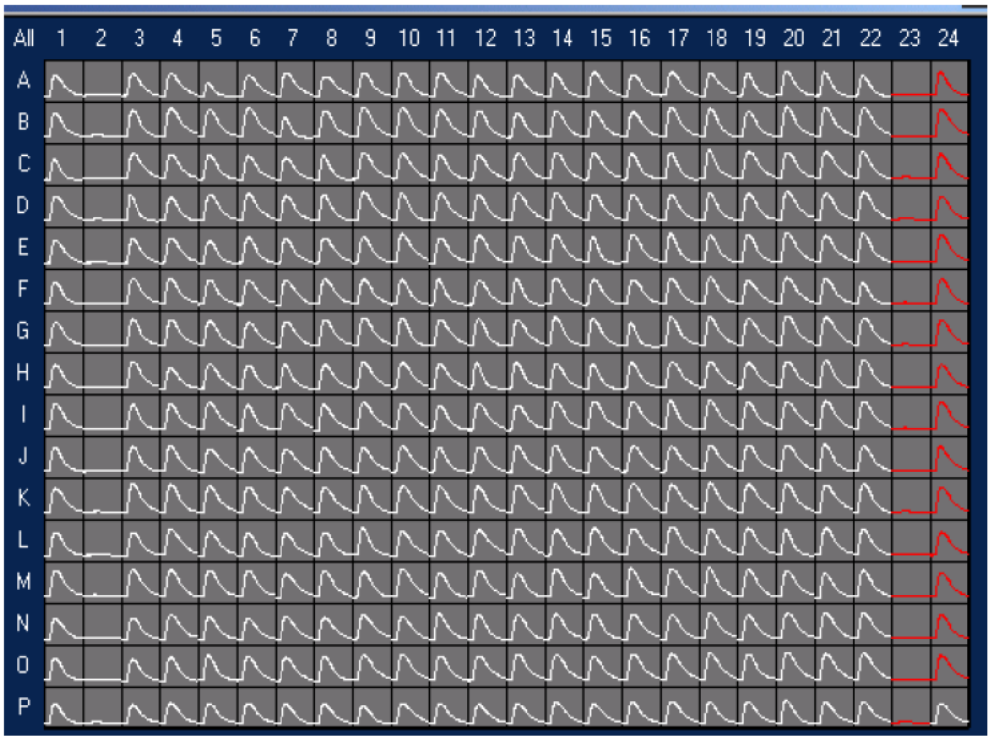

Figure 15. Establishment of calcium transient assay for the screening of GPR142 antagonist

(A) Dose-response activation of human GPR142 expressing cells against Trp in calcium transient assay measured on FLIPR TETRA.

(B) The Z' factor value was 0.63 with limited numbers (n = 16) of positive (high, 1 mM Trp) and negative (low, no Trp) controls shown in graph with red.

(A)

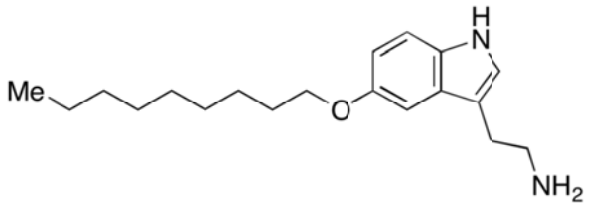

(B)

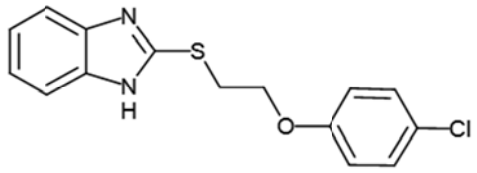

(C)

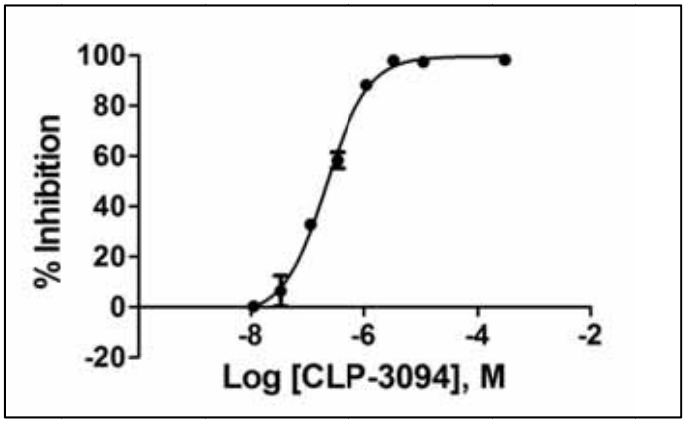

Figure 16. Identification of antagonists of GPR142 from HTS

(A) Structure of NOT (5-(nonyloxy)tryptamine), Serotonin (5-HT1D) selective agonist.

(B) Structure of CLP-3094.

(C)Antagonist activity of CLP-3094. HEK293 cells transiently expressing mouse GPR142 were incubated with CLP-3094 at the indicated concentrations for 30 min before being stimulated with 200 μM Trp for 90 min at 37°C. The data are presented as means of % inhibition from quadruplicate measurements with standard deviation shown as error bars.

(A)

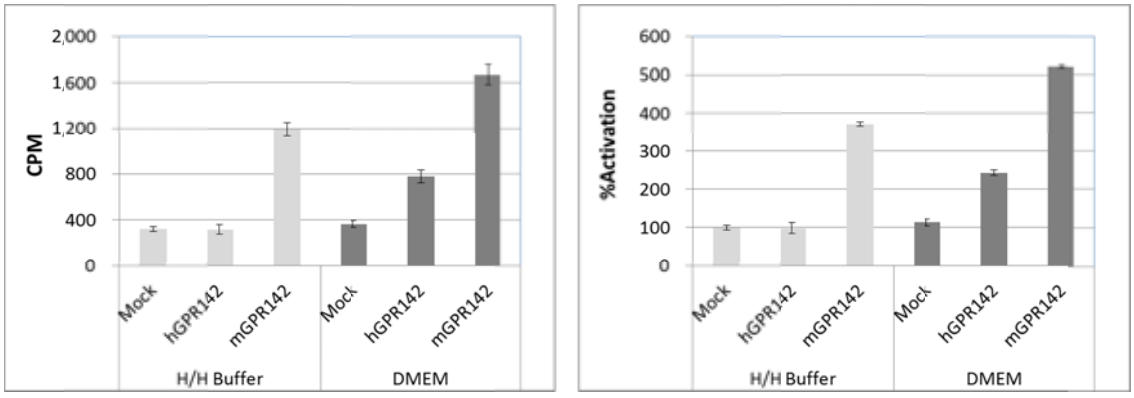

(B)

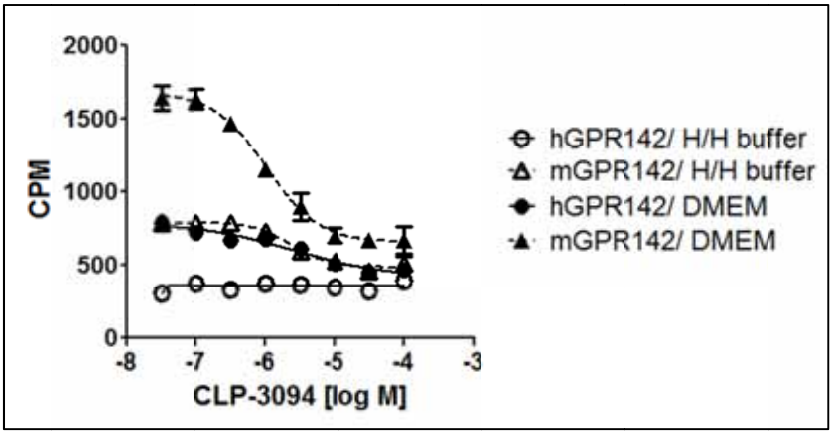

Figure 17. Inverse antagonism of CLP-3094

(A) Over-expression of GPR142 leads to constitutive inositol phosphate accumulation in HEK293 cells. The horizontal/first axis shows the plasmids transfected, and buffer used for the assay. The data are presented as means from quadruplicate measurements with standard deviation shown as error bars.

(B) Inverse agonist activity of CLP-3094. HEK293 cells transiently expressing mouse GPR142 were incubated with CLP-3094 at the indicated concentrations for 30 min before accumulation with assay buffer (DMEM or H/H buffer) with no additional Trp for 90 min at 37°C. The data are presented as means from quadruplicate measurements with standard deviation shown as error bars.

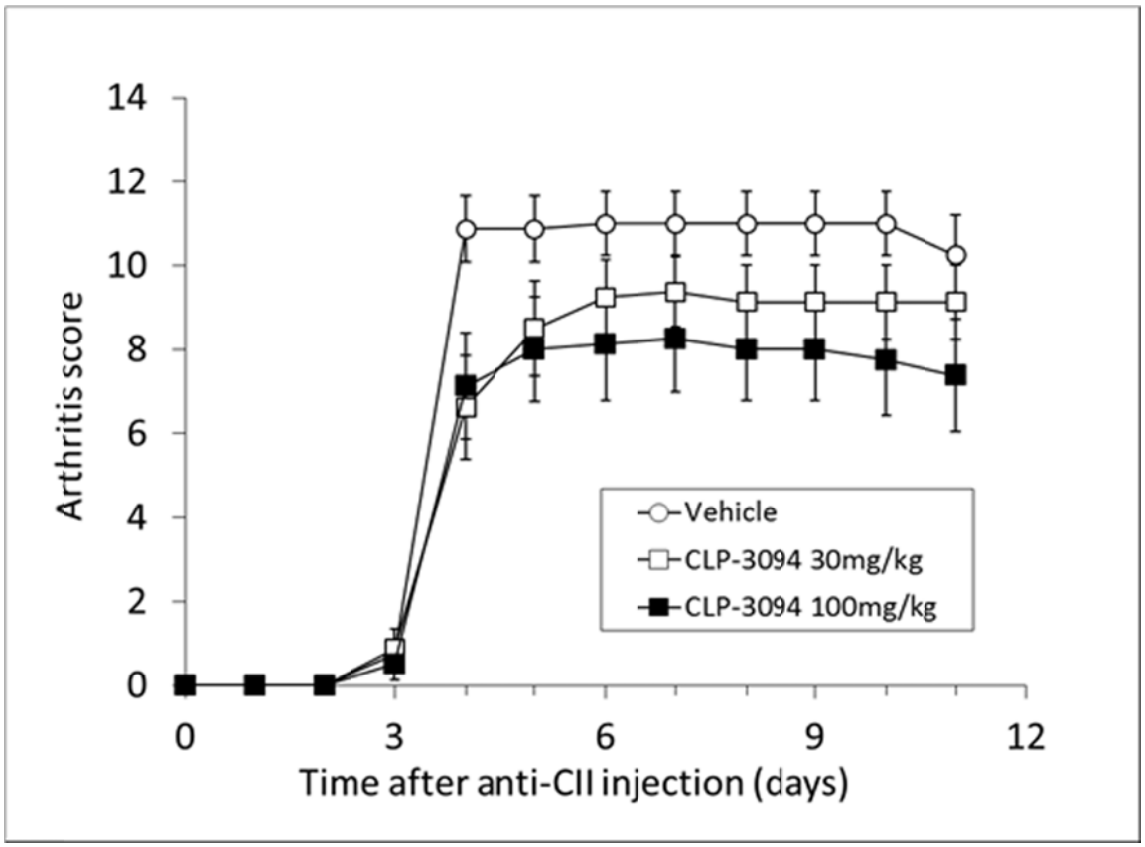

Figure 18. Reduced severity of arthritis by CLP-3094 administration to CAIA mice following collagen antibody induced arthritis induction

Groups of 8 C57Bl/6 mice were treated via i.v. on Day 0 with 2 mg anti-CII antibody and subsequently boosted with 100 μg of LPS on Day 3 to induce collagen induced antibody arthritis. CLP-3094 was i.p. administered daily from Day 0 to Day 11. Arthritis scores are shown as mean (S.E.M.). Open circle: vehicle treated control; Square: CLP-3094 (Open: 30 mg/kg, Closed: 100 mg/kg) administrated.

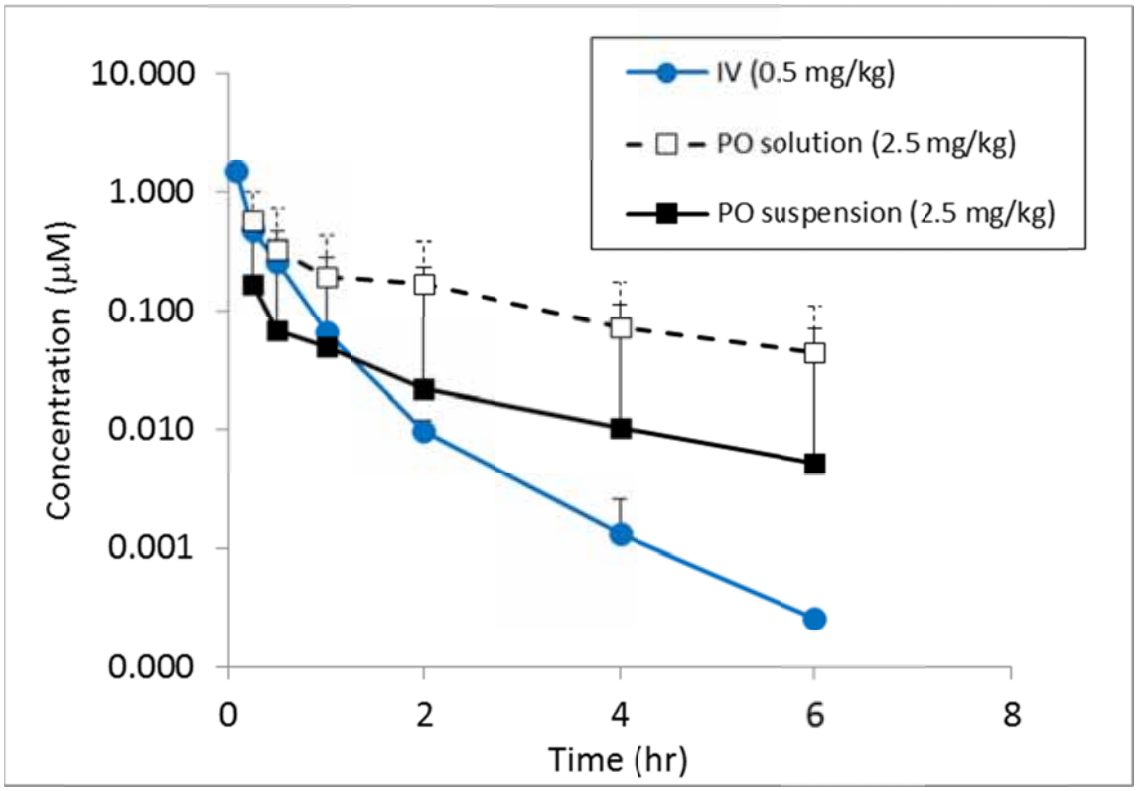

Figure 19. PK profiles after intravenous or oral administration of CLP-3094 to mice

Groups of 3 male C57Bl/6 were treated with CLP-3094 intravenously (0.5 mg/10 mL/kg) or orally (2.5 mg/20 mL/kg as the solution in DMSO/Tween 80/saline (10/10/80, v/v/v) or 2.5 mg/20 mL/kg as the suspension in 0.5% methylcellulose solution). Closed circle: IV administrated; Open square: PO as the solution ; Closed square: PO as the suspension.

Plasma concentration of CLP-3094 are shown as mean (S.E.M.).

Table 2. Selectivity of antagonist activity of CLP-3094.

GPCR	GPR142*	GPR139*	GHSR*	CCR4*	MT1**	5-HT1**
Ligand	L-Tryptophan	Surrogate Agonist	Ghrelin	MDC / CCL22	Melatonin	Serotonin
IC_{50}	0.2 μM	1.67 μM	N.D.	N.D.	>50 μM	>50 μM
Efficacy	100%	30%	N.D.	N.D.	N.D.	N.D.

*N.D. = Not Determined
*Aequorin assay using stable cell line
**GTPγs binding assay using cell membrane

Summary of antagonist pharmacology (IC_{50}) of CLP-3094 determined in intracellular aequorin assay or GTPγs binding assay. A GTPγs binding assay was performed using membrane purchased from Euroscreen S.A., and following the manufacturer's instructions. Briefly, membranes were incubated with ^{35}S labeled GTPγ and compounds at room temperature for 60 minutes. Then, suspended WGA SPA beads (1 mg/well) were added, and the plates were sealed and incubated for more than one hour at room temperature. They were then centrifuged at 200 *g* and plate luminescence was measured in a Wallac Microbeta® Trilux.

Table 3. In vitro metabolic stability, solubility and plasma protein binding ratio of CLP-3094

A) Metabolic stability

Protein concentration	Protein	Reaction time	Residual rates (%)	Midazolam residual rates (%)
1.0 mg/mL	Rat-S9	5 min	26.8	69.3
1.0 mg/mL	Rat-S9	15 min	2.2	50.5
1.0 mg/mL	Rat-S9	30 min	1.2	34.7
1.0 mg/mL	Mouse-S9	5 min	0.4	53.4

B) Solubility

Solution	Solubility (μM)
JP1	>100.0
JP2	0.7

C) Plasma protein binding

Protein Source	Protein Type	Binding (%)	Free(%)
Mouse-Plasma	C57BL/6J	99.76	0.24

Table 4. PK parameters after intravenous or oral administration of CLP-3094 to mice

iv (0.5 mg/kg, solution (DMSO/Tween80/Saline =10/10/80))

Parameters	Mean	SD
AUC0-inf (μM*h)	0.567	0.078
t1/2 (h)	0.74	0.363
CL (mL/min/kg)	48.9	6.9
Vss (L/kg)	0.981	0.261

po (2.5 mg/kg, solution (DMSO/Tween80/Saline =10/10/80))

Parameters	Mean	SD
Cmax (μM)	0.584	0.426
AUC0-inf (μM*h)	1.01	1.23
tmax (h)	0.25	0.00
t1/2 (h)	1.71	0.47
Bioavailability (%)	35.5	43.5

po (2.5 mg/kg, suspension (0.5%MC))

Parameters	Mean	SD
Cmax (μM)	0.170	0.011
AUC0-inf (μM*h)	0.180	0.038
tmax (h)	0.25	0.00
t1/2 (h)	1.93	0.30
Bioavailability (%)	6.35	1.36

Table 5. Comparison of CAIA and CIA model

	Collagen Antibody-Induced Arthritis; CAIA	Collagen-Induced Arthritis; CIA
Experimental period	7～14 days	6～8 week
Mouse strain	C57BL/6、DBA1、Balb/c、Transgenic、etc	DBA/1、C57BL/6
Method of administration	Intraperitoneal, tail vein administration	Intradermal administration near the base of the tail
Arthritis incidence	100%	60～90%
Arthritis score	10～16	6～12
Arthritis Induction	arthritogenic mAb cocktail、LPS	Type II collagen、Adjuvant

CHAPTER 4

Concluding Remarks

GPR142, a putative amino acid receptor, is expressed in pancreatic islets and immune cells, but the physiological role of this receptor remains unclear. Synthetic GPR142 agonists were demonstrated to stimulate glucose-dependent insulin secretion and improve glucose tolerance in vivo (15). In the course of finding the GPR142 endogenous ligand, I found an agonistic activity against GPR142 in extract of porcine brain, discriminated from Trp.

In Chapter 2, I purified the active component(s) from the porcine brain extract to identify the compound that causes the agonistic activity against GPR142. From ion peak patterns observed in the mass spectrum and the comparison of the activity profiles, it was concluded that the agonistic activity against GPR142 observed in porcine brain extract was caused by zinc ion. Further analysis revealed that zinc acts not as a ligand (agonist), but as a modulator that changes the properties of receptor activation by both natural and surrogate ligands.

In Chapter 3, CLP-3094 was found to be a novel, potent, selective GPR142 antagonist. I also showed the pharmacological characteristics of CLP-3094. GPR142 KO mice were shown to be protected from anti-type II collagen (CII) antibody-induced arthritis and dextran sulfate sodium (DSS)-induced colitis. Administration of CLP-3094 reduced the arthritis scores dose-dependently, but not by much. The hypothesis that increased production of inflammatory cytokines might accelerate the degradation of L-Tryptophan, which decreases the desensitization of GPR142, corresponds reasonably well with the experimental data. But, further examination of GPR142 remains to be performed before truly understanding how GPR142 is involved in regulation of the pathogenesis and development of inflammatory diseases.

It is my hope that this work will contribute to the evolution of drugs for providing good medications to patients in the future.

Acknowledgments

I would like to express my deep gratitude to all those who provided guidance, support and encouragement during the preparation of this dissertation.

Most of all, I would like to express my sincere thanks to Professor Akiyoshi Fukamizu for his valuable guidance and encouragement in this study.

I also would like to express my gratitude to all collaborators and coworkers for their leading me in the appropriate direction throughout my research work. Especially, I would like to note the invaluable assistance given by Dr. Futoshi Nara. Without his guidance and persistent help this thesis would not have been possible.

I am deeply indebted to Drs. Hiroaki Maeda, Nobuaki Watanabe, Hideyuki Shiozawa, Satoshi Nishimura, Harumi Kuwabara and Miyuki Nagasaki for their teaching about purification of natural ligands, *in vivo* experimental techniques and for their discussions.

Finally, I appreciate greatly the support of my daughter and my husband.

References

1. Wettschureck N, Offermanns S.: Mammalian G proteins and their cell type specific functions. Physiological Reviews 2005 Oct, 85 (4): 1159–204.

2. Exton JH.: Regulation of phosphoinositide phospholipases by hormones, neurotransmitters, and other agonists linked to G proteins. Annu Rev Pharmacol Toxicol. 1996, 36: 481–509.

3. Sunahara RK, Dessauer CW, and Gilman AG.: Complexity and diversity of mammalian adenylyl cyclases. Annu Rev Pharmacol Toxicol. 1996 36: 461–480.

4. Dhanasekaran N and Dermott JM.: Signaling by the G12 class of G proteins. Cell Signal 1996, 8: 235–245.

5. Buhl AM, Johnson NL, Dhanasekaran N, and Johnson GL.: G alpha 12 and G alpha 13 stimulate Rho-dependent stress fiber formation and focal adhesion assembly. J Biol Chem 1995, 270: 24631–24634.

6. Andrew L. Hopkins & Colin R. Groom: The druggable genome. Nature Reviews Drug Discovery 1, 2002 Sep, 727-730.

7. IMS Health World Review: IMS Industry Ranking of the Top 100 Products. IMS Health, Fairfield, CT, USA(2000)

8. Libert F, Parmentier M, Lefort A, Dinsart C, Van Sande J, Maenhaut C, et al. Selective amplification and cloning of four new members of the G protein-coupled receptor family. Science. 1989, 244:569–572.

9. Vassilatis DK, Hohmann JG, Zeng H, Li F, Ranchalis JE, Mortrud MT, et al. The G protein-coupled receptor repertoires of human and mouse. Proc Natl Acad Sci USA. 2003, 100:4903–4908.

10. Libert F, Vassart G, Parmentier M. Current developments in G-protein-coupled receptors. Curr Opin Cell Biol. 1991, 3:218–223.

11. Kotarsky K, Nilsson NE.: Reverse pharmacology and the de-orphanization of 7TM receptors. Drug Discov Today Technol. 2004 Oct, 1(2):99-104.

12. Henderson G, McKnight AT. The orphan opioid receptor and its endogenous ligand—nociceptin/orphanin FQ. Trends Pharmacol Sci. 1997;18:293–30.

13. Fredriksson R., Hoglund PJ., Gloriam DE., Lagerstrom MC., Schioth HB.: Seven evolutionarily conserved human rhodopsin G protein-coupled receptors lacking close relatives. FEBS Lett. 2003 Nov, 554 (3): 381–8.

14. Liu C., Bonaventure P., Lee G., Nepomuceno D., Kuei C., Wu J., Li Q., Joseph V., Sutton SW., Eckert W., Yao X., Yieh L., Dvorak C., Carruthers N., Coate H., Yun S., Dugovic C., Harrington A., Lovenberg TW.: GPR139, an Orphan Receptor Highly Enriched in the Habenula and Septum, Is Activated by the Essential Amino Acids L-Tryptophan and L-Phenylalanine. Mol. Pharmacol. (2015) 88 November 1: 911-925.

15. Lizarzaburu M., Turcotte S., Du X., Duquette J., Fu A., Houze J., Li L., Liu J., Murakoshi M., Oda K., Okuyama R., Nara F., Reagan J., Yu M., Medina JC.: Discovery and optimization of a novel series of GPR142 agonists for the treatment of type 2 diabetes mellitus. Bioorganic & Medicinal Chemistry Letters (2012) 22: 5942–5947.

16. Matsuo, A.,Matsumoto,S.,Nagano,M.,Masumoto,K.H.,Takasaki,J.,Matsumoto, M.,et al.: Molecular cloning and characterization of a novel Gq-coupled orphan receptor GPRg1 exclusively expressed in the central nervous system. Biochem. Biophys.Res.Commun. (2005) 331, 363–369.

17. Süsens, U.,Hermans-Borgmeyer,I.,Urny,J.,andSchaller,H.C.: Characterisation and differential expression of two very closely related G-protein-coupled receptors,GPR139 and GPR142, in mouse tissue and during mouse development. Neuropharmacology (2006) 50, 512–520.

18. Kirsten BA,, Jens LJ., Morten H., Garrick P,S. and Gunnar PHD.: Protection of primary dopaminergic midbrain neurons by GPR139 agonists supports different mechanisms of MPPC and rotenone toxicity. Frontiers in Cellular Neuroscience (2016) 10 (164), 1-10.

19. Xiong Y., Motani A., Reagan J., Gao X., Yang H., Ma J., Schwandner R., Zhang Y., Liu q., Miao L., Luo J., Tian H., Chen J-L., Murakoshi M., Nara F., Yeh WC., Cao Z. manuscript is in preparation.

20. Moffett JR, Namboodiri MA.: Tryptophan and the immune response. Immunol Cell Biol. (2003) 81 Aug;(4):247-65.

21. Shajib MS, Khan WI.: The role of serotonin and its receptors in activation of immune responses and inflammation. Acta Physiol (Oxf). (2015) 213 Mar;(3): 561-74.

22. Bosma-den Boer, M.M., Wetten, M.L., Pruimboom, L.: Chronic inflammatory diseases are stimulated by current lifestyle: how diet, stress levels and medication prevent our body from recovering. Nutrition and Metabolism. (2012)9 (32), 1-14.

23. Scott DL., Wolfe F., Huizinga TW.: Rheumatoid arthritis. Lancet (2010) 376 (9746): 1094–108.

24. "Handout on Health: Rheumatoid Arthritis". National Institute of Arthritis and Musculoskeletal and Skin Diseases. August 2014. Retrieved July 2, 2015.

25. Funk JL., Cordaro. L., Wei H., Benjamin JB., Yocum DE.: Synovium as a source of increased amino-terminal parathyroid hormone-related protein expression in rheumatoid arthritis. A possible role for locally produced parathyroid hormone-related protein in the pathogenesis of rheumatoid arthritis. J Clin Invest. (1998) 101 : 1362-1371.

26. Parekh RB., Dwek. RA., Sutton BJ., Fernandes DL., Leung A., Stanworth D., Rademacher TW., Mizuochi T., Taniguchi T., Matsuta K., et al.: Association of rheumatoid arthritis and primary osteoarthritis with changes in the glycosylation pattern of total serum IgG. Nature (1985) 316 : 452-457.

27. Steinitz M., Izak. G., Cohen S., Ehrenfeld M., Flechner I.: Continuous production of monoclonal rheumatoid factor by EBV-transformed lymphocytes. Nature (1980) 287 : 443-445.

28. Paulus HE., Oh M., Sharp JT., Gold RH., Wong WK., Park GS., Bulpitt KJ.: Western Consortium of Praticing Rheumatologists. Correlation of single time-point damage scores with observed progression of radiographic damage during the first 6 years of rheumatoid arthritis. J Rheumatol. (2003) 30 : 705-713.

29. Ziolkowska M., Kurowska M., Radzikowska A., Luszczykiewicz G., Wiland P., Dziewczopolski W., Filipowicz-Sosnowska A., Pazdur J, Szechinski J., Kowalczewski J., Rell-Bakalarska M., Maslinski W.: High levels of osteoprotegerin and soluble receptor activator of nuclear factor kappa B ligand in serum of rheumatoid arthritis patients and their normalization after anti-tumor necrosis factor alpha treatment. Arthritis Rheum. (2002) 46 :1744-1753.

30. Lewandowicz J., Dabkowska B., Nowak D.: Influence of gold salts treatment on the serum concentration of IL-1 and IL-2 in patients with rheumatoid arthritis. Arch Immunol Ther Exp (Warsz). (1995) 43 : 195-198.

31. Furst DE., Dromgoole SH., Desiraju RK., Paulus HE: Clinical pharmacology of tolmetin :comparisons in rheumatoid arthritis patients and normal volunteers. J Clin Pharmacol. (1983) 23 : 329-335.

32. Szyper-Kravitz M.: The hemophagocytic syndrome/macrophage activation syndrome: a final common pathway of a cytokine storm. Isr Medr Assoc J. (2009) 11 : 633-634.

33. Caplazi P., Baca M., Barck K., Carano RAD., DeVoss J., Lee WP.,Bolon B., Diehl L.: Mouse Models of Rheumatoid Arthritis. Vet Pathol September (2015) 52: 819-826

34. Cook AD., Rowley MJ., Stockman A., et al.: Specificity of antibodies to type II collagen in early rheumatoid arthritis. J Rheumatol. (1994) 21:1186–1191

35. Schurgers E., Billiau A., Matthys P.: Collagen-induced arthritis as an animal model for rheumatoid arthritis: focus on interferon-g. J Interferon Cytokine Res. (2011) 31:917–926.

36. Park MJ., Park HS., Oh HJ., et al.: IL-17-deficient allogeneic bone marrow transplantation prevents the induction of collageninduced arthritis in DBA/1J mice. Exp Mol Med. (2012) 44: 694–705.

37. Sarkar S., Justa S., Brucks M., et al.: Interleukin (IL)-17A, F and AF in inflammation: a study in collagen-induced arthritis and rheumatoid arthritis. Clin Exp Immunol. (2014) 177:652–661

38. Schurgers E., Billiau A., Matthys P.: Collagen-induced arthritis as an animal model for rheumatoid arthritis: focus on interferon-g. J Interferon Cytokine Res. (2011) 31:917–926.

39. Nandakumar KS., Holmdahl R.: Collagen antibody-induced arthritis. Methods Mol Med. (2007) 136:215–223.

40. Komatsu N., Takayanagi H.: Inflammation and bone destruction in arthritis: synergistic activity of immune and mesenchymal cells in joints.Front Immunol. (2012) Apr 13;3:77.

41. Nandakumar KS., Svensson L., Holmdahl R.: Collagen type II-specific monoclonal antibody-induced arthritis in mice: description of the disease and the influence of age, sex, and genes. Am J Pathol. (2003) 163:1827–1837.

42. Hirose J., Tanaka S.: [Animal models for bone and joint disease. CIA, CAIA model].[Article in Japanese]Clin Calcium. (2011) Feb;21(2):253-9.

43. Nandakumar KS., Ba¨cklund J., Vestberg M, et al.: Collagen type II (CII)-specific antibodies induce arthritis in the absence of T or B cells but the arthritis progression is enhanced by CII-reactive T cells. Arthritis Res Ther. (2004) 6:R544–R550.

44. Ranges GE., Sriram S., Cooper, S M. : Prevention of type II collagen-induced arthritis by in vivo treatment with anti-L3T4. J. Exp. Med. (1985)162, 1105–1110.

45. Chung S, Funakoshi T, and Civelli O: Orphan GPCR research. Br J Pharmacol. 2008 Mar; 153(Suppl 1): S339–S346.

46. Kojima M, Hosoda H, Date Y, Nakazato M, Matsuo H, Kangawa K: Ghrelin is a growth-hormone-releasing acylated peptide from stomach. Nature (1999), Dec 9; 402(6762):656-60.

47. Philip E. Brandish, Lorraine A. Hill, Wei Zheng, and Edward M. Scolnick: Scintillation proximity assay of inositol phosphates in cell extracts: High-throughput measurement ofG-protein-coupled receptor activation. Analytical Biochemistry 313 (2003) 311–318

48. Songzhu An, Gene Cutler, Jack Jiagang Zhao, Shu-Gui Huang, Hui Tian, Wanbo Li, Lingming Liang, Miki Rich, Amy Bakleh, Juan Du, Jin-Long Chen, and Kang Dai: Identification and characterization of a melanin-concentrating hormone receptor. Proc. Natl Acad. Sci. USA (2001) 98: 7576−7581.

49. MANUFACTURER'S GUIDE (**卓上脱塩装置　マイクロ･アシライザー　技術資料集**)

50. T Badessa, V Shaposhnik: The electrodialysis of electrolyte solutions of multi-charged cations. Journal of Membrane Science (2016), 498: 86–93

51. Holst B, Egerod KL, Schild E, Vickers SP, Cheetham S, Gerlach LO, Storjohann L,Stidsen CE, Jones R, Beck-Sickinger AG, Schwartz TW: GPR39 signaling is stimulated
by zinc ions but not by obestatin. Endocrinology (2007), 148: 13-20

52. Muller A, Kleinau G, Piechowski CL, Muller TD, Finan B, Pratzka J, Gruters A, Krude H, Tschop M, Biebermann H: G-protein coupled receptor 83 (GPR83) signaling determined by constitutive and zinc(II)-induced activity. PLoS One (2013), 8:e53347

53. Dabbaghmanesh MH, Taheri Boshrooyeh H, Kalantarhormozi MR, Ranjbar Omrani GhH: Assessment of Zinc Concentration in Random Samples of the Adult Population in Shiraz, Iran. Iran Red Crescent Med J (2011), 13(4): 249-255

54. Murakoshi M, Kuwabara H, Nagasaki M, Xiong YM, Reagan JD, Maeda H, Nara F.: Discovery and pharmacological effects of a novel GPR142 antagonist.J Recept Signal Transduct Res.(2016), Nov 3:1-7. [Epub ahead of print]

55.Chausmer AB.: Zinc, insulin and diabetes. J Am Coll Nutr (1998) 17(2), 109–115.

56.Tallman DL, Taylor CG.: Potential interactions of zinc in the neuroendocrine-endocrine disturbances of diabetes mellitus type 2. Can J Physiol Parmacol (1999) 77, 919–933.

57. Abe-Ohya R, Ishikawa T, Shiozawa H, Suda K, Nara F.: Identification of metals from osteoblastic ST-2 cell supernatants as novel OGR1 agonists. J Recept Signal Transduct Res. 2015 Oct;35(5): 485-92

58. Ananthanarayanan VS, Kerman A: Role of metal ions in ligand-receptor interaction: insights from structural studies. Mol Cell Endocrinol (2006): 246: 53-9

59. Parker MS, Wong YY, Parker SL.: An ion-responsive motif in the second transmembrane segment of rhodopsin-like receptors. Amino Acids (2008) 35: 1–15

60. Swaminath G, Steenhuis J, Kobilka B, Lee TW.: Allosteric Modulation of β2-Adrenergic Receptor by Zn2+. Mol Pharmacol. (2002) Jan;61(1): 65-72.

62. Barrondo S, Salles J: Allosteric modulation of 5-HT(1A) receptors by zinc: Binding studies. Neuropharmacology (2009) 56: 455-462.

63. D. Lambert,Ed., Calcium Signaling Protocols (Methods in Molecular Biology, Volume 114) (1999) 125-133.

64. Terato, K., K. A. Hasty, R. A. Reife, M. A. Cremer, A. H. Kang, J. M. Stuart.: Induction of arthritis with monoclonal antibodies to collagen. J. Immunol. (1992) 148: 2103.

65. Terato, K., D. S. Harper, M. M. Griffiths, D. L. Hasty, X. J. Ye, M. A. Cremer, J. M. Seyer.: Collagen-induced arthritis in mice: synergistic effect of E. coli lipopolysaccharide bypasses epitope specificity in the induction of arthritis with monoclonal antibodies to type II collagen. Autoimmunity (1995) 22: 137.

66. Kagari, T., H. Doi, T. Shimozato.: The importance of IL-1β and TNF-α, and the noninvolvement of IL-6, in the development of monoclonal antibody-induced arthritis. J. Immunol. (2002) 169:1459.

67. Kanauchi, O., T. Nakamura, K. Agata, K. Mitsuyama, and T. Iwanaga. 1998. Effects of germinated barley foodstuff on dextran sulfate sodium-induced colitis in rats. J. Gastroenterol. 33: 179–188

68. Widner B., Werner ER., Schennach H., Fuchs D.: An HPLC method to determine tryptophan and kynurenine in serum simultaneously. Adv Exp Med Biol. (1999) 467: 827-32.

69. Zhang, J. H., Chung, T. D., and Oldenburg, K. R.: A Simple Statistical Parameter for Use in Evaluation and Validation of High Throughput Screening Assays, J Biomol Screen (1999) 4, 67-73.

70. Tiberi M and Caron MG (1994) High agonist-independent activity is a distinguishing feature of the dopamine D1B receptor subtype. J Biol Chem 269:27925–27931.

71. Milligan G, Bond RA, and Lee M (1995) Inverse agonism: pharmacological curiosity or potential therapeutic strategy? Trends Pharmacol Sci 16:10–13

72. Comai S, Bertazzo A, Carretti N, Podfigurna-Stopa A,Luisi S, and Costa C.V.L.(2010) Serum Levels of Tryptophan, 5-Hydroxytryptophan and Serotonin in Patients Affected with Different Forms of Amenorrhea. Int J Tryptophan Res. 2010; 3: 69–75.

73. Brian M. Campbell, Erik Charych, Anna W. Lee, Thomas Möller : Kynurenines in CNS disease: regulation by inflammatory cytokines. Front Neurosci (2014) 6;8:12.

74. Aarsland TI., Landaas ET., Hegvik TA., Ulvik A., Halmøy A., Ueland PM., Haavik J.: Serum concentrations of kynurenines in adult patients with attention-deficit hyperactivity disorder (ADHD): a case–control study. Behav Brain Funct. (2015) Nov 5;11(1):36.

75. Hu LA., Tang PM., Eslahi NK., Zhou T., Barbosa J., Liu Q.: Identification of surrogate agonists and antagonists for orphan G-protein-coupled receptor GPR139. J Biomol Screen. (2009) Aug;14(7):789-97.

76. Wang J., Zhu LY., Liu Q., Hentzer M., Smith GP., Wang MW.: High-throughput screening of antagonists for the orphan G-protein coupled receptor GPR139. Acta Pharmacol Sin. (2015) Jul;36(7):874-8.

77. Coombs JH., Bloom BJ., Breedveld FC., Fletcher MP., Gruben D., Kremer JM., Burgos-Vargas R., Wilkinson B., Zerbini CA., Zwillich SH.: Improved pain, physical functioning and health status in patients with rheumatoid arthritis treated with CP-690,550, an orally active Janus kinase (JAK) inhibitor: results from a randomised, double-blind, placebo-controlled trial. Ann Rheum Dis. (2010) 69: 413-6.

78. Billich A.: Drug evaluation: apilimod, an oral IL-12/IL-23 inhibitor for the treatment of autoimmune diseases and common variable immunodeficiency. IDrugs. (2007) 10: 53-9.

79. McCluggage LK., Scholtz JM.: Golimumab: a tumor necrosis factor alpha inhibitor for the treatment of rheumatoid arthritis. Ann Pharmacother. (2010) 44: 135-44.

80. Nandakumar KS, Bäcklund J, Vestberg M, et al. Collagen type II (CII)-specific antibodies induce arthritis in the absence of T or B cells but the arthritis progression is enhanced by CII-reactive T cells. Arthritis Res Ther. (2004) 6: 544–550.

81. Gainetdinov RR., Premont RT., Bohn LM., Lefkowitz RJ., Caron MG.: Desensitization of G protein-coupled receptors and neuronal functions. Annu Rev Neurosci. (2004) 27:107-44.